

# Delineating the Role of GxxxG Motif in Amyloidogenesis: A New Perspective in Targeting Amyloid-Beta Mediated AD Pathogenesis

Dibakar Sarkar and Anirban Bhunia\*



Cite This: *ACS Bio Med Chem Au* 2024, 4, 4–19



Read Online

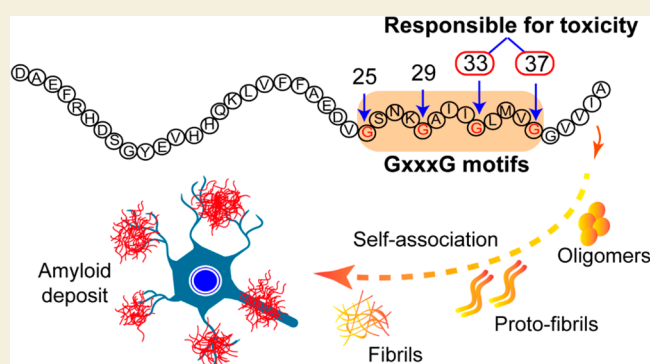
ACCESS |

Metrics & More

Article Recommendations

**ABSTRACT:** The pursuit of a novel structural motif that can shed light on the key functional attributes is a primary focus in the study of protein folding disorders. Decades of research on Alzheimer's disease (AD) have centered on the Amyloid  $\beta$  ( $A\beta$ ) pathway, highlighting its significance in understanding the disorder. The diversity in the  $A\beta$  pathway and the possible silent tracks which are yet to discover, makes it exceedingly intimidating to the interdisciplinary scientific community. Over the course of AD research,  $A\beta$  has consistently been at the forefront of scientific inquiry and discussion. In this review, we epitomize the role of a potential structural motif (GxxxG motif) that may provide a new horizon to the  $A\beta$  conflict. We emphasize on how comprehensive understanding of this motif from a structure–function perspective may pave the way for designing novel therapeutics intervention in AD and related diseases.

**KEYWORDS:** APP,  $A\beta$ , AV20, GxxxG motif, helix–helix association, oligomer, structural dynamicity, ion-channel-like pore, mutation, toxicity



## INTRODUCTION

Alzheimer's disease (AD) is a severe neurodegenerative disorder, characterized by progressive impairment of cognitive function and memory loss. To date, there are over 45.0 million AD cases worldwide, enlisting it as the fifth most prevalent cause of death on a global scale and the number is growing at an alarming rate.<sup>1</sup> By 2050, the number of individuals with dementia is expected to cross over 120 million.<sup>2</sup> On top of that, the emotional and financial burden on patients, their families, and communities are enormous. Although over 25 amyloid-forming proteins have been identified and linked to various severe diseases, AD stands out as the most important of them.<sup>3</sup> This distinction arises from its extensive prevalence within the aging population, highlighting its prominence as a significant global health concern. The landscape of AD and dementia-related mortality is intricate, with numerous confounding factors contributing to the overall picture, including age, gender, advanced disease severity, and comorbid conditions such as diabetes, hypertension, coronary artery disease, and cerebrovascular disease. Comprehending the intricate interplay between disease severity and mortality is indispensable for predicting long-term outcomes and evaluating the effectiveness of novel therapeutic interventions. Given the extended timeframes involved, assessing these long-term effects often presents challenges within the framework of randomized controlled trials. As of now, the accumulation of

amyloid-beta ( $A\beta$ ) peptide into extracellular amyloid plaques is considered to be the distinct morphological hallmark of AD.<sup>4–8</sup> However, the in-depth molecular mechanism of  $A\beta$  pathway driving AD pathogenesis is still unclear. Over the years, significant findings on the proteolytic processing of amyloid precursor protein (APP),<sup>9–12</sup> potential evidence of highly toxic transient  $A\beta$  oligomers,<sup>13–19</sup> and presence of high degree of polymorphism<sup>20–24</sup> in fibril structures have created an intricate scenario.

In this rapidly evolving landscape, the conserved GxxxG motifs present in the C-terminus of  $A\beta$  appears to be a noteworthy target. Here, we present a systematic and cross-disciplinary state-of-the-art update of the translational research based on biophysical, structural, and cellular data that substantiate the crucial role of well-designed GxxxG motifs in the biological spectrum of  $A\beta$ 40/42. We provide a comprehensive and evidence-based overview of recent developments in the understanding of the regulatory role played by the GxxxG motif at different temporal scales. Lastly,

**Received:** August 16, 2023

**Revised:** October 18, 2023

**Accepted:** October 18, 2023

**Published:** October 31, 2023



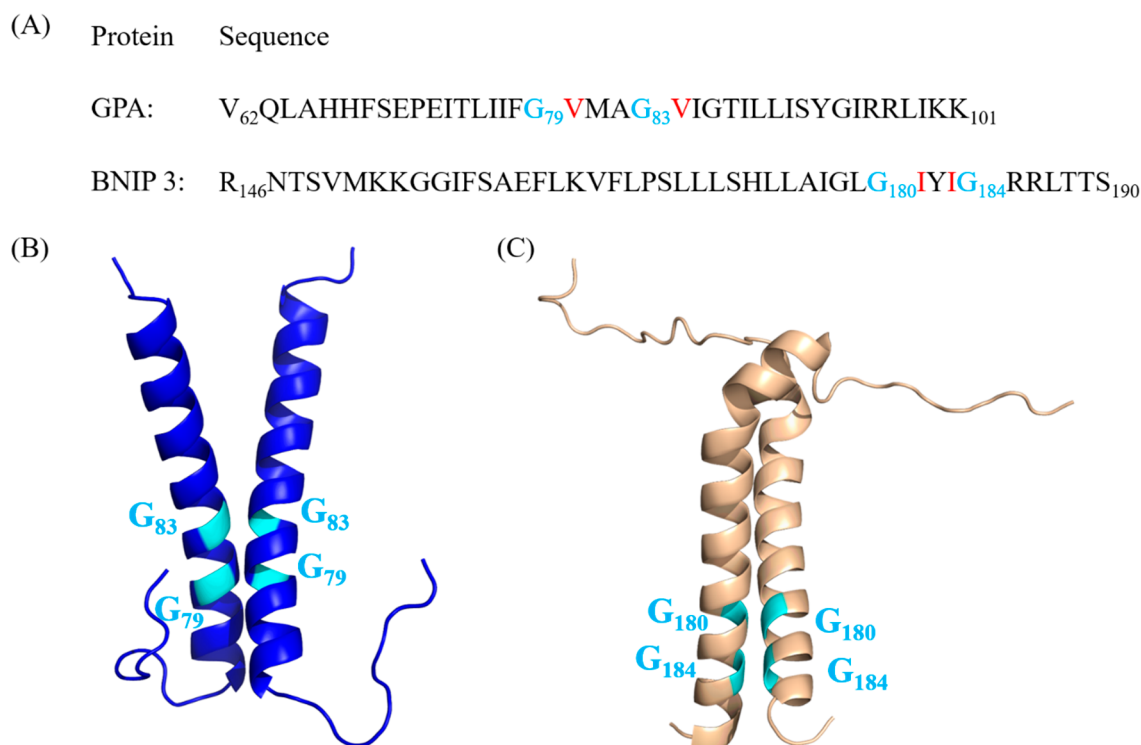


**Figure 1.** (A) Amino acid sequence of TM domain of GPA and BNIP3 containing GxxxG motif. The neighboring  $\beta$ -branched residues are highlighted (red). Helix–Helix association in (B) GPA (PDB file: 1AFO), and (C) BNIP3 (PDB file: 2J5D) homodimer mediated by GxxxG motif. Gly residues within the GxxxG motif are highlighted with a cyan color.

we highlight recent developments in designing short peptide-based agents targeting such motif and their future prospects regarding  $A\beta$  peptide inhibition, providing potential therapeutic avenues for AD.

### LESSONS LEARNED FROM GXXXG-MEDIATED HELIX–HELIX INTERACTIONS

The GxxxG motif stands out as the most prevalent sequence motif in naturally occurring transmembrane (TM) proteins and some soluble proteins that comprise at least one  $\alpha$ -helix.<sup>25</sup> These TM motifs are essential for engaging in oligomeric interactions. Interestingly, Gly residues within a GxxxG motif exhibit a higher degree of conservation compared to random Gly residues. The three residue spacing allows the Gly residues in a GxxxG motif to lie on one face of the helix.<sup>25,26</sup> The lack of side chain in Gly allows the two helices to come into close proximity, thereby increasing van-der-Waals forces between adjacent helices, stabilizing the helix–helix association and thus forming a helical dimer. The flat surface provided by the Gly residues can offer a wide range of specific interactions that can manifest around the GxxxG motifs. The presence of  $\beta$ -branched amino acids such as Val, Ile, and Thr, often found at adjacent positions (as shown in Figure 1A), facilitates Gly to act as a molecular notch, thereby strengthening the helix–helix interactions.<sup>27</sup> The GxxxG motif therefore can be considered as a framework for the dimerization of TM  $\alpha$ -helices.

Although the GxxxG motifs are abundant in human transmembrane domain (TMD) sequences, the extent to which these motifs participate in TMD interactions remains inconclusive. With the limited number of studies, one can only assume certain role in TM helix–helix dimerization. For example, a conserved GxxxG motif situated in the distinctive

membrane-spanning segment of the mitochondrial ATP synthase is involved in the dimerization via inter- and intramolecular TMD interactions.<sup>28</sup> The glycophorin A (GPA) is one of the most well-characterized model protein that offers insights into the conformation and behavior of intramembranous segments in single-pass transmembrane proteins.<sup>29</sup> The TM domain largely consists of hydrophobic amino acid residues. By using solution NMR, MacKenzie et al.<sup>30</sup> showed that the interaction surface consists of two ridges and their corresponding groove. The side chains of V80 and V84 form one ridge that packs against the groove created by G79 and G83 of the opposite monomer (Figure 1B). The findings from site-directed mutagenesis and solution NMR spectroscopy collectively indicate that these Gly residues stabilize dimerization by providing a surface for packing, allowing helix proximity and by entropic effects.<sup>30,31</sup> The GxxxG motif therefore seems to be the most essential component of the GPA interaction motif. Similarly, the proapoptotic protein BNIP3 (Bcl-2 Nineteen-kDa interacting protein 3) comprising a GxxxG motif, has also been found to form the right-handed parallel TM dimer.<sup>32</sup> Solution NMR study showed that the dimer is stabilized by hydrophobic side chain contacts of A176, I177, I181, and I183 and tight packing due to the presence of A176, G180, and G184 in the sequence spanning  $-A_{176}\text{xxx}G_{180}\text{xxx}G_{184}-$  residues (Figure 1C).<sup>33</sup> This motif also appears to play a vital role in aligning the side chains within the His–Ser node, which is necessary for the formation of hydrogen bonds. In addition, the aromatic residues F157, F161, and F165 forms a hydrophobic cluster which is stabilized by intra- and intermonomeric stacking interactions. Computational analysis has suggested that Gly residues are essential at certain positions not only to serve as hydrogen bonding donors but also for reducing the steric hindrance for larger side-chain

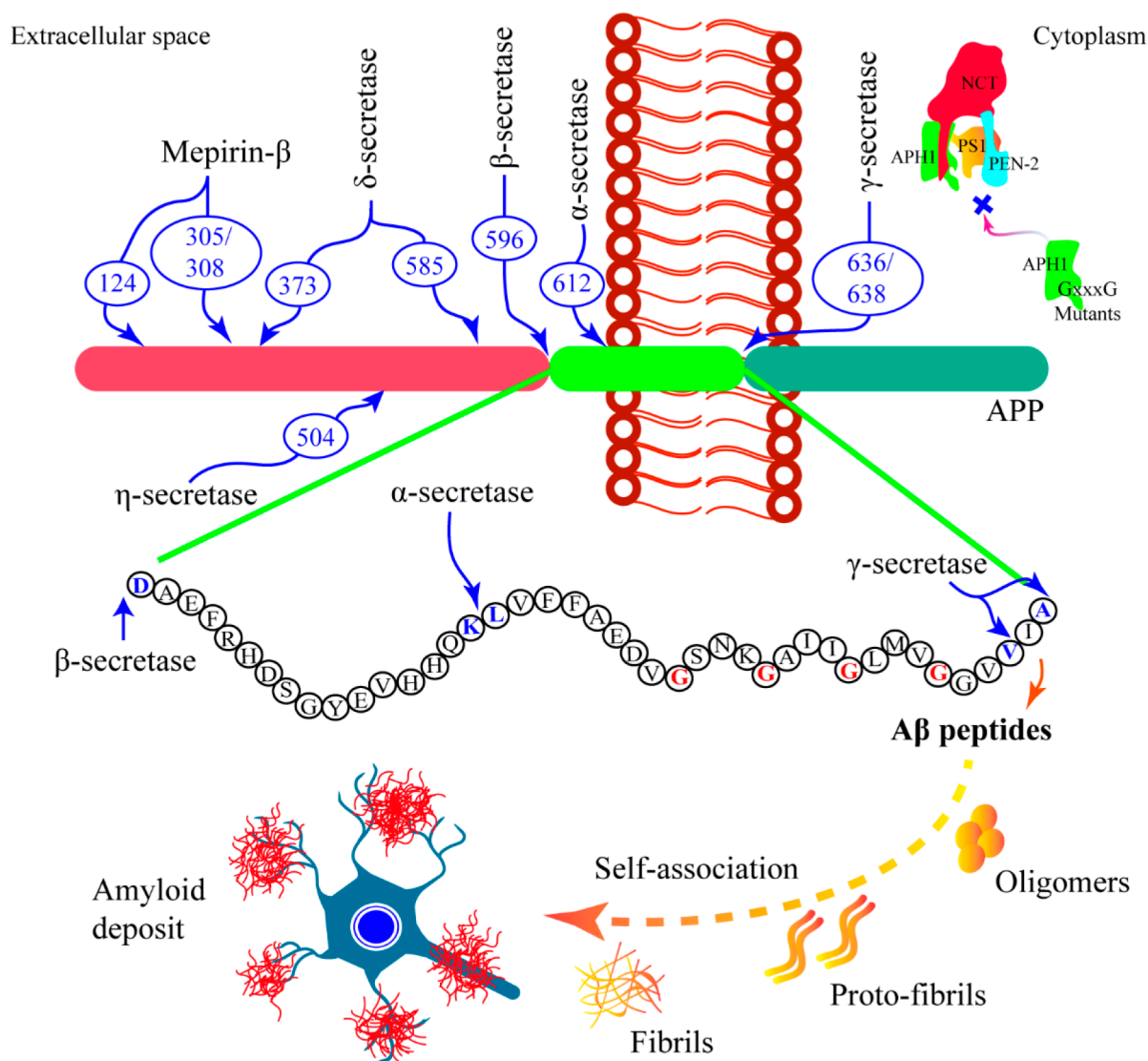


**Figure 2.**  $A\beta$  pathway involving APP processing, generation of  $A\beta$  peptides of various length followed by amyloid deposition via multiple steps. Blue arrows indicate APP cleavage sites by different proteolytic enzymes. Glycine residues from GxxxG motifs are marked in red. Numbering follows the sequence of APP695.

amino acids at neighboring positions; Thus, providing a rational structural understanding for the prevalence of GxxxG motifs in TM homodimers.<sup>34</sup> Several other proteins containing the GxxxG motifs have been identified as crucial structural components. For example, the GxxxG/A motifs present in the TMDs of Human  $\text{Na}^+$ /Taurocholate Co-Transporting Polypeptide (NTCP) plays crucial role in cellular processes. Particularly, mutation in the  $\text{G}_{233}\text{LxxxG}_{237}\text{L}$  (TMD7) motif displayed reduced interaction with wild-type NTCP and impaired membrane expression, bile acid transport activity, highlighting its importance for proper folding and sorting of NTCP, as well as its HBV/HDV receptor function.<sup>35</sup> Similarly, the TMDs of major histocompatibility complex (MHC) class II molecules contain multiple highly conserved GxxxG dimerization motifs, and research has shown that the pairing of these motifs plays a crucial role in defining distinct MHC class II conformers.<sup>36</sup> Using the 11–5.2 monoclonal antibody (mAb), which exhibits selective binding to I-A<sup>k</sup> class II molecules, it was observed that the single GxxxG motif in the molecule's  $\beta$  chain interacts with the N-terminal M1 GxxxG motif situated within the I-A<sup>k</sup>  $\alpha$  chain.<sup>37</sup> Furthermore, it was

noted that the binding of the Tü36 mAb is specifically hindered by mutations in the M1  $\alpha$  chain GxxxG motif, highlighting potential structural and functional differences.<sup>38</sup>

A striking similarity between these segment and Alzheimer's  $A\beta$  peptide (UniProt accession ID of Amyloid Precursor protein (P05067)) is that both can form helical dimer in the presence of membrane mimicking detergent-micelle.<sup>39,40</sup> The hydrophobic environment of a lipid bilayer, which facilitates hydrogen bonding is likely to promote dimerization. It is noteworthy to mention that many TM proteins have been identified to be dimeric in nature, with TM segments resembling those found in both GPA and APP. Therefore, it is reasonable to speculate that APP, which also possess analogous GxxxG segments within its TM domain, exists as a dimer in the lipid bilayer.<sup>41–43</sup> Studies have shown substantial evidence of SDS-stable dimeric configurations for both  $A\beta_{40}$  and  $A\beta_{42}$ , suggesting that these  $A\beta$  dimers are linked with the lipid raft domains within the membrane.<sup>39,44</sup> In this context, we can assume that when APP is sequentially processed, its TM domains retain their association, forming dimeric  $A\beta$  peptides just as they existed in the intact APP molecules.

However, the impacts of these intramembranous peptides are likely dependent on their site of generation and duration within the lipid bilayer, necessitating further investigation to fully comprehend their functional implications in Alzheimer's disease.

### ■ INFLUENCE ON APP PROCESSING AND SUBSEQUENT A $\beta$ PRODUCTION

From proteolytic generation to accumulation into amyloid, the A $\beta$  pathway has always been the center of attraction in AD pathophysiology (Figure 2). Typically, the proteolytic cleavage of APP by  $\beta$ - and  $\gamma$ -secretases within the lipid bilayer generates A $\beta$  peptides with predominant lengths of 40 (A $\beta$ 40) and 42 (A $\beta$ 42) amino acids.<sup>45</sup> APP is first cleaved by  $\beta$ -secretase, resulting in a 99-residue membrane-anchored fragment ( $\beta$ CTF or C99), which is then processed by  $\gamma$ -secretase to generate A $\beta$  peptides. However, escalating number of proteolytic enzymes capable of cleaving APP and similar molecules suggest that A $\beta$  peptides could also be produced in mechanisms other than through the coordinated actions of  $\beta$ - and  $\gamma$ -secretases.<sup>46,47</sup> Nevertheless, a large number of the studies are focused on the  $\gamma$ -secretase complex, which mainly consist of presenilins (PS), anterior pharynx defective 1 (APH-1), nicastrin (NCT), and presenilin enhancer 2 (PEN-2).<sup>48,49</sup> It is generally accepted that after the cleavage by  $\gamma$ -secretases, a large amount of A $\beta$  peptides jump from membrane to the extracellular space. The charged and polar amino acids at the N-terminus wield sufficient drag to pull the remaining hydrophobic region through the lipid bilayer and into the aqueous medium.<sup>50</sup>

In this context, the role played by the GxxxG motifs have been investigated by several groups.<sup>51–55</sup> Munter et al. showed that the  $\gamma$ -secretase cleavages of APP are intricately connected to the strength of dimerization within the substrate transmembrane segments (TMS) and these motifs are liable for facilitating the production of highly toxic A $\beta$ 42.<sup>51</sup> Mutation of the consecutive G<sub>29</sub>xxxG<sub>33</sub>xxxG<sub>37</sub> motifs by Leu or Ile was found to reduce the A $\beta$ 40 and A $\beta$ 42 production drastically.<sup>56</sup> Interestingly, the mammalian multipass membrane protein APH-1 also contains a conserved transmembrane G<sub>122</sub>xxxG<sub>126</sub>xxxG<sub>130</sub> motif that partake in helix–helix association and is crucial for the stable binding of APH-1 with presenilin, nicastrin, and PEN-2, collectively forming the  $\gamma$ -secretase complex.<sup>55</sup> Thus, the interaction between APP and other proteins within the  $\gamma$ -secretase complex is likely to be influenced by the GxxxG motif.

Several familial mutations in APP such as A21G (Flemish), E22G (Arctic), E22Q (Dutch), and D23N (Iowa), have been found to influence the proteolytic processing of APP and associated A $\beta$  production.<sup>57–61</sup> Among these mutations, the A21G mutation appears to be particularly intriguing as A21G mutation introduces a fourth consecutive upstream GxxxG motif. The A21G mutation was found to have a strong influence on intramembranous processing by the  $\gamma$ -secretase complex and increases the A $\beta$  production by approximately 2-fold.<sup>61</sup> A study by Tzu-Chun Tang et al. revealed that A21G mutation induce conformational changes in the structure of C55, the first 55 residues of the  $\beta$ -CTF which subsequently leads to an increased A $\beta$  production.<sup>62</sup> Interestingly, the A21 residue resides at a breakpoint between a well-defined  $\beta$ -strand and the TM helix of  $\beta$ -CTF. The introduction of an additional GxxxG motif by A21G mutation destabilizes the  $\beta$ -sheet structure and increases the  $\alpha$ -helical structure of the G<sub>25</sub>xxxG<sub>29</sub> sequence, thereby stabilizing the TM dimers through GxxxG

motifs.<sup>62,63</sup> Conversely, Ala substitutions in the GxxxG motif of  $\beta$ -CTF causes decrease in the level of longer A $\beta$  species such as A $\beta$ 42 and A $\beta$ 43 and a concomitant increase in shorter A $\beta$  (i.e., A $\beta$ 34, A $\beta$ 35, A $\beta$ 37, and A $\beta$ 38) production.<sup>51,64</sup>

### Regulation of A $\beta$ Aggregation and Subsequent Neurotoxicity

The GxxxG repeated motif from the C-terminus represent a unique feature of APP as well as of A $\beta$  peptides. Structurally, this motif plays an important role in stabilizing both helix–helix association and sheet-to-sheet packing. Typically, the two Gly residues of the GxxxG motif are placed on the same side of a TM helix or on the same face of a  $\beta$ -sheet. The nonchiral nature and small side-chain of Gly offer flexibility, contributing to peptide dynamism and facilitating membrane insertion through pore formation. Recent studies have shown that several amyloid fibrils, including those linked with AD take parallel in-register  $\beta$ -sheet, where Gly can create molecular notches or grooves on the surface of the  $\beta$ -sheet, extending along the length of the amyloid fibril.<sup>65–68</sup> The secondary conformation of the GxxxG motifs are thought to be highly dependent on the surrounding residues (i.e., hydrophobic or polar). Solid-state NMR analysis of A $\beta$ 40 and A $\beta$ 42 peptides has revealed that the G<sub>25</sub>xxxG<sub>29</sub> motif, which includes polar amino acids within its sequence, is a constituent of a  $\beta$ -hairpin structure.<sup>69</sup> However, the second and third GxxxG motifs in the A $\beta$  peptides surrounded by hydrophobic  $\beta$ -branched residues adopt  $\beta$ -strand or  $\beta$ -sheet secondary structure.<sup>70</sup> Ahmed et al. showed that the solvent accessible turns at H13-Q15, G25-G29, and G37-G38 facilitate the compact folding of the peptide, by placing F19 in contact with L34.<sup>71</sup> NMR derived structural models have shown that in both A $\beta$ 40 and A $\beta$ 42, the surface grooves formed by G33 and G37 can stabilize sheet-to-sheet packing by providing space for large amino acid side chains.<sup>72</sup> Moreover, computational studies have revealed that Gly to Leu substitutions at positions 33 and 37 within A $\beta$ 42 leads to a notable increase in the conformational instability.<sup>73</sup>

Interestingly, the three consecutive GxxxG motifs present in the TM sequence of prion protein (PrP) have significant role in organization of transmembrane helices and packaging of amyloid fibers (Figure 3).<sup>26,74</sup> The formation of ion channels by both toxic A $\beta$  peptides and PrP peptides, which ultimately leads to neuronal cell death, suggests a possible common pathological role for these motifs.<sup>75–78</sup> Notably, the incidence of such structural motif in a number of bacterial channel proteins that induce ion channel formation further support the ion channel hypothesis.<sup>79,80</sup> By G  $\rightarrow$  L substitution in A $\beta$ , specifically the G37L mutation, Kim et al.<sup>81</sup> demonstrated the importance of the Gly residues of the consecutive GxxxG motif, particularly the G37 in pore formation in synthetic membranes and inducing toxicity in Neuro 2a neuroblastoma cells. Later Hung et al.<sup>82</sup> reported that the GxxxG repeat motif significantly modulate the formation of toxic A $\beta$  oligomers. G  $\rightarrow$  L mutants of A $\beta$ 42, generally termed as GSL peptides (G25L, G29L, G33L or G37L) showed increased rate in amyloid formation and a decrease in the formation of toxic oligomeric species. When treated against primary mouse cortical neurons, all mutants showed lower toxicity compared to the wild type (WT) A $\beta$ , with the G33L and G37L substitutions demonstrating the most significant reduction in toxicity, suggesting a direct correlation with oligomer formation. Harmeier et al.<sup>83</sup> reported that substitutions at

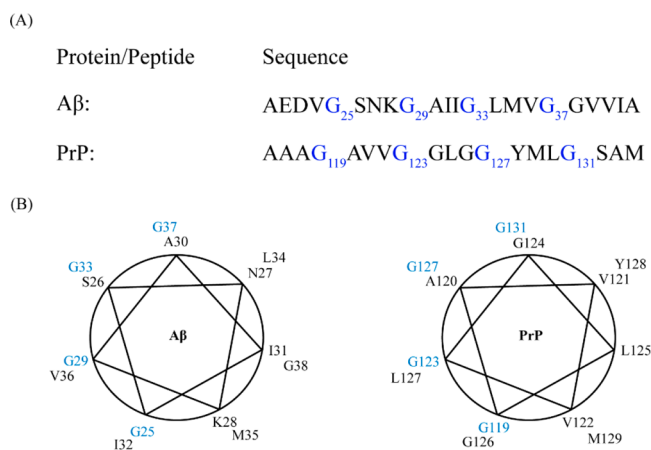


**Figure 3.** (A) Three consecutive GxxxG motif present in the C-terminus of A $\beta$  and prion protein. (B) Helical wheel projection displaying the resemblance in the distribution of the GxxxG motif between A $\beta$  (25–38) and PrP (119–131) sequences. The similarity between these two sequences indicates a common role in pathophysiology.

G33 of A $\beta$ 42 by Ala or Ile dramatically reduced toxicity in neuroblastoma cells and while generating higher molecular weight oligomers in vitro. They showed that unlike WT A $\beta$ , G33-substituted A $\beta$  could not hinder hippocampal long-term potentiation (LTP) or interfere with eye development in a transgenic *Drosophila* model. Mutation at G37 of A $\beta$ 42 by Val also exhibited a substantial reduction in the toxicity. Although it did not enhance the aggregation kinetics significantly, but it led to the formation of a distinct ellipse-like aggregate morphology.<sup>84</sup> In addition to various models such as cell dysfunction, cell death, synaptic alteration, or tau phosphorylation the G37L substitution was further tested in a transgenic *C. elegans* model.<sup>85</sup> The A $\beta$  G37L was actually found antitoxic, thereby supporting the GxxxG-mediated A $\beta$  oligomer formation hypothesis.

### MECHANISTIC INSIGHT INTO THE GXXXG-MODULATED AMYLOIDOGENESIS

A thorough comprehension of amyloid aggregation necessitates insight into the aggregation-prone domains embedded within the peptide sequence. Extensive research has shed light on two essential motifs: (1) the central hydrophobic KLVFF sequence and the (2) GxxxG motifs. The KLVFF sequence occupies a central role in A $\beta$  aggregation by serving as a key recognition site for self-assembly. It promotes the formation of the characteristic cross- $\beta$  sheet structure, offering structural stability to the aggregates. Alternatively, the GxxxG motif facilitates structural dynamism, prolonging the lifetime of toxic oligomers, and is crucial for cellular toxicity. Together, these motifs contribute significantly to our understanding of the multifaceted nature of amyloid aggregation dynamics. Recently, we have demonstrated the distinctive nature of the GxxxG repeating motifs in the C-terminal of A $\beta$  fragment A21-V40 (AV20) peptide, illustrating their role in preserving structural flexibility and subsequent neurotoxicity (Figure 4).<sup>86</sup> Point mutation of these crucial Gly residues modulates the hydrogen bond networking, influencing the helix–helix association and thereby intervening in differential fibrillation pathways. We found that the G  $\rightarrow$  L mutation in the C-terminal GxxxG motif resulted in a dramatic increase in the

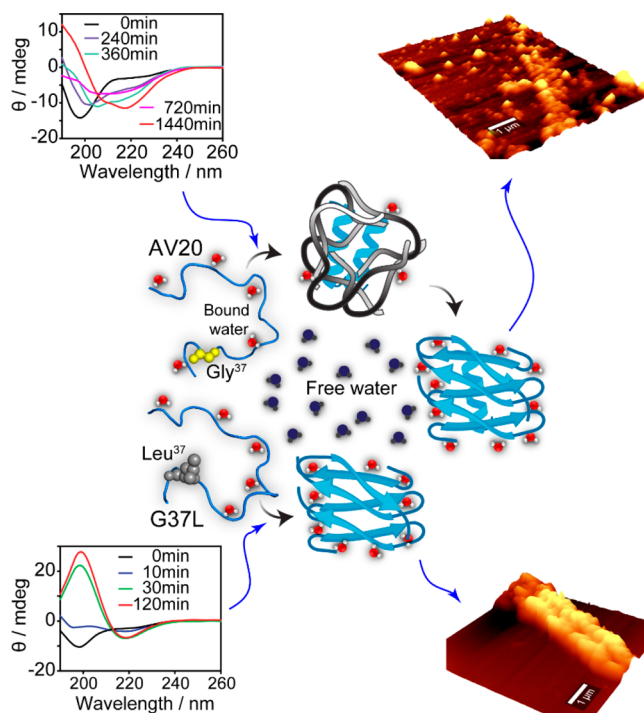


**Figure 4.** Mechanistic insight into the GxxxG-mediated amyloid formation of C-terminal A $\beta$  fragment. The WT peptide showed cylindrical oligomers with partial helical secondary conformation. The G37L mutant on the other hand exhibited compact fibrillar structure with  $\beta$ -sheet conformation. Reproduced from ref 86 with permission from John Wiley & Sons, ©2019 Wiley-VCH Verlag GmbH & Co. KGaA, Weinheim.

aggregation kinetics. Remarkably, as the G  $\rightarrow$  L substitution was shifted toward the C-terminus, a notable reduction in aggregate size heterogeneity was observed. This finding highlights the significant role of these Gly residues in modulating both the rate of aggregation and the distribution of aggregate sizes. Furthermore, we showed that the toxicity against neuronal SHSY5Y cells decreases significantly as substitution with Leu approaches the C-terminal. Thus, the GxxxG motif contributed to a greater conformational heterogeneity which subsequently reflected on the cytotoxicity, whereas mutation leads to a fast transition from random coil to  $\beta$ -sheet conformation. Additionally, hydrogen bonding networks played a crucial role in the selection of conformation. Substitution by Leu residue destabilizes the intermediate conformers by preventing the hydrogen bond formation and hence reduces its neurotoxicity. This corroborates well with the current shift in the focus toward the prefibrillar species owing to their functional involvement in disease pathophysiology.

Our recent investigation employing solvent relaxation NMR has unveiled the pivotal role of solvent dynamics in distinguishing the aggregation pathway among diverse peptides (Figure 5A).<sup>87</sup> Notably, we made an intriguing discovery regarding the impact of the Gly to Leu mutation on solvent dynamics, resulting in a strikingly altered aggregation pathway. Solvent relaxation NMR in combination with Molecular Dynamics (MD) simulation revealed that substantial structural transition in A $\beta$ 40 occurred in the early stage of aggregation, in which water molecules actively participated in the nucleation event. Our findings indicated that higher temperature conditions resulted in a faster rate of structural transition, as

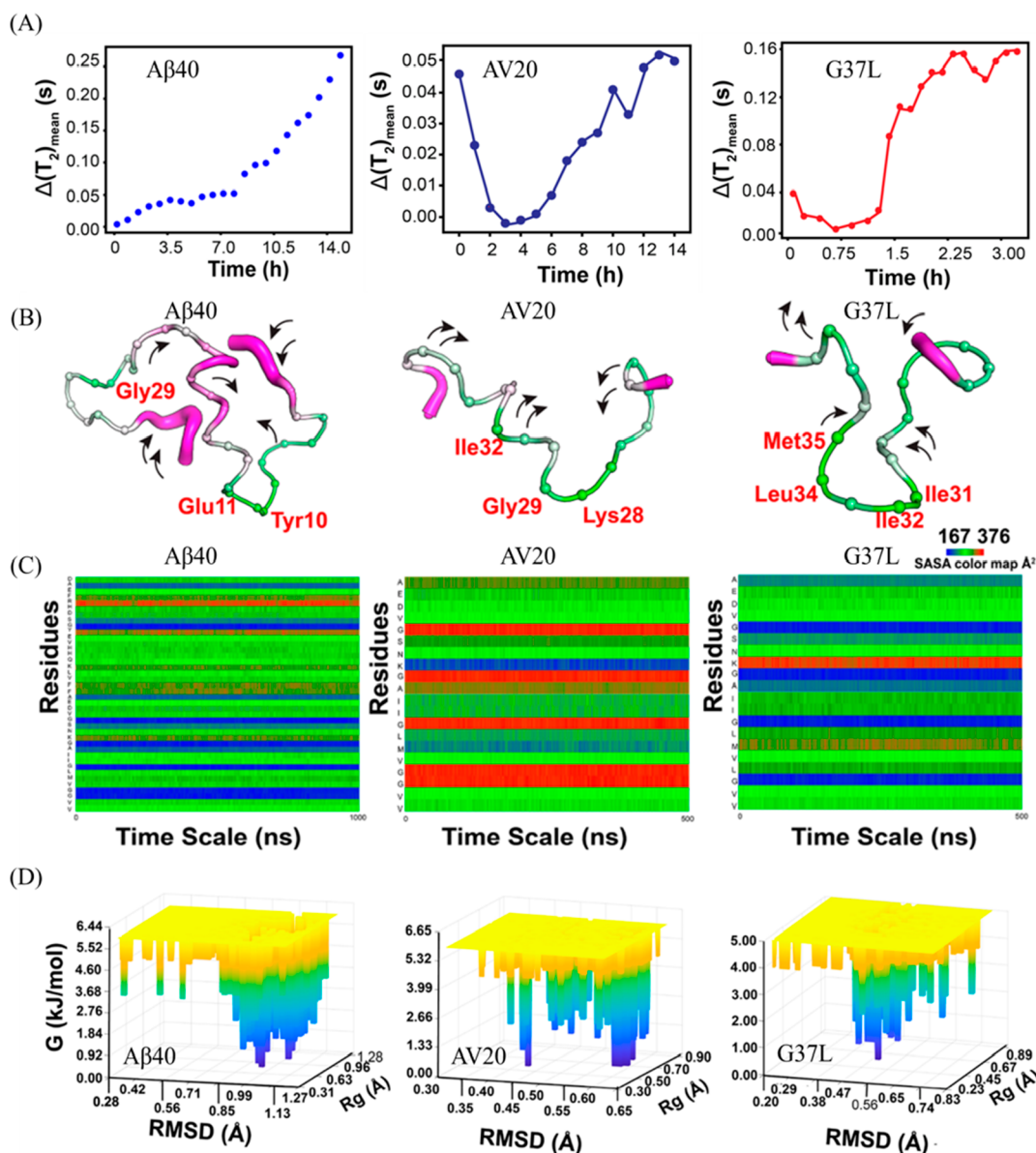


**Figure 5.** (A)  $\Delta(T_2)_{\text{mean}}$  (s) versus time (h) of A $\beta$ 40 (160  $\mu\text{M}$ ), AV20 (160  $\mu\text{M}$ ) and G37L (80  $\mu\text{M}$ ) sample (pH  $\sim$  7.4) incubated at 37  $^\circ\text{C}$ .  $\Delta(T_2)_{\text{mean}} = (T_2)_{\text{mean}}(t) - (T_2)_{\text{mean}}(t_{\text{min}})$ , where  $(T_2)_{\text{mean}}(t_{\text{min}})$  denotes the lowest  $(T_2)_{\text{mean}}$  value. (B) Dynamic profiles of A $\beta$ 40, AV20, and G37L peptide residues in classical simulations. Cartoon putty representation with green to magenta color scheme indicating lowest to highest fluctuations. C $\alpha$  atoms shown as spheres, highlighting residues with the least fluctuation. Arrows represent average drift (motion) during simulation. (C) Deconvoluted values of solvent accessible surface area (SASA) for individual residues of A $\beta$ 40, AV20, and G37L measured using collective variables, root-mean squared deviation (RMSD), and radius of gyration (Rg). (D) Gibbs free energy landscape of A $\beta$ 40, AV20, and G37L measured using collective variables, root-mean squared deviation (RMSD), and radius of gyration (Rg). Reprinted with permission from ref 87. Copyright 2021 American Chemical Society.

evidenced by the faster saturation of the relaxation time parameter ( $\Delta(T_2)_{\text{mean}}$ ). From a thermodynamic perspective, this implies that the activation energy required for the structural transition is lower at higher temperatures. In other words, the increased thermal energy at higher temperatures facilitates the conformational changes and promotes the transition to more compact structures. This observation provides valuable insights into the thermodynamic aspects of the structural evolution of the system and contributes to our understanding of the temperature-dependent dynamics of the aggregation process. In contrast to A $\beta$ 40, AV20 (A21-V40 of A $\beta$ 40) exhibited a distinct transverse or  $T_2$  relaxation profile, indicating notable differences in its dynamics during the fibrillation process. Moreover, AV20 demonstrated conver-

gence and stability at an early time scale during MD simulation. The changes in the number of water molecules and H-bonding water within the hydration shell showed a pattern consistent with reduced solvent accessibility and hydrophobic collapse in AV20. Furthermore, AV20 demonstrated a higher activation energy threshold for fibrillation initiation, suggesting a greater resistance to spontaneous aggregation compared to A $\beta$ 40. However, the introduction of external factors such as agitation or other extrinsic influences can overcome this threshold and induce fibrillation in AV20.

The G  $\rightarrow$  L mutation in G37L affects solvent accessibility and dynamics, leading to faster exclusion of “bound” water. Additional insights were obtained from the solvent-accessible surface area (SASA) analysis, revealing differences in solvent

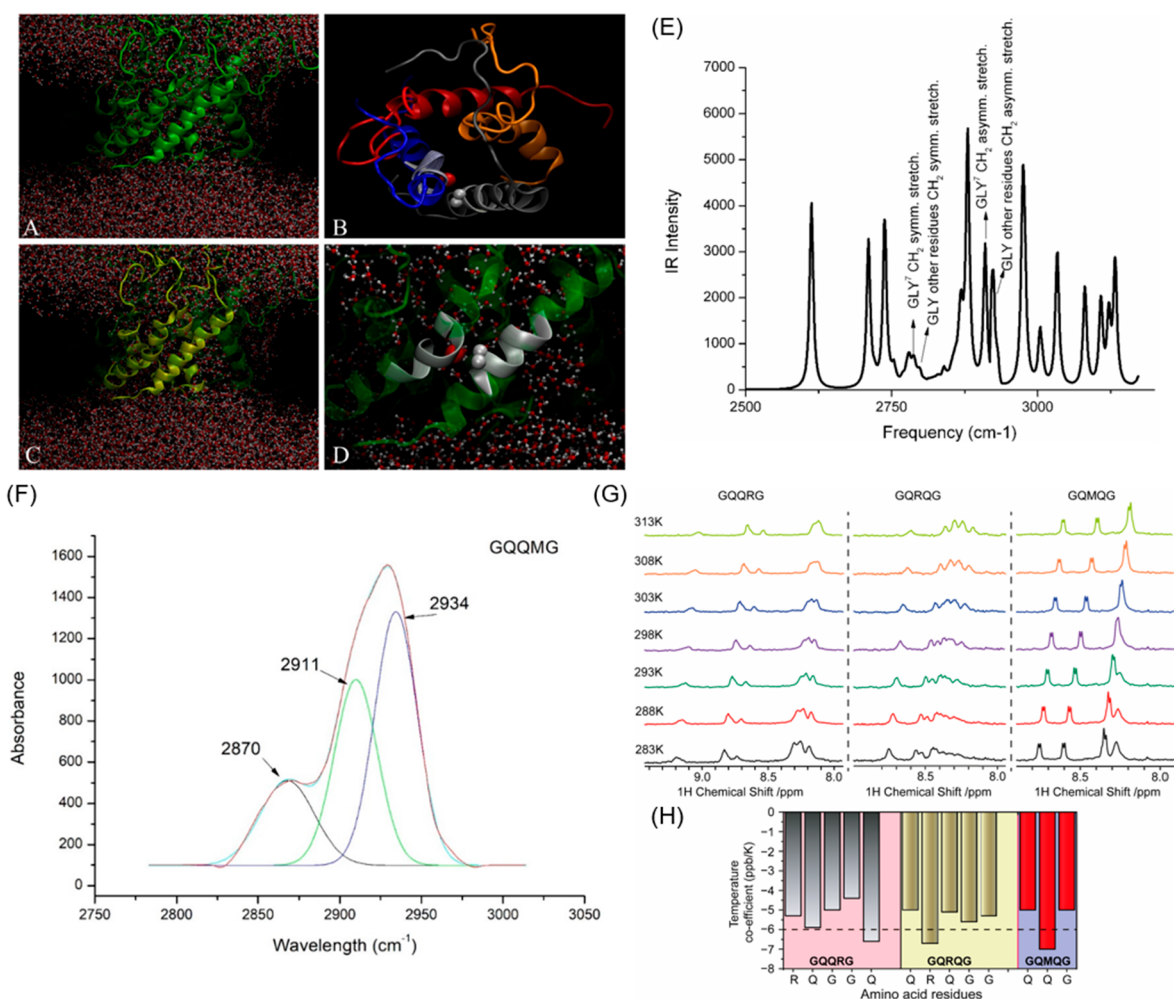


**Figure 6.** (A) An ion-channel-like pore is formed by a 24-mer of  $A\beta$  (1–40) embedded within a POPC bilayer, allowing water to cross the bilayer. (B) A top-down of the tetramer ion-channel-like pore. (C) The tetramer organizes into a structured pore. (D) Two intersecting  $\alpha$ -helices within the tetramer create an angle of  $39 \pm 5$  degrees, with gray spheres symbolizing the two  $C\alpha$ -hydrogens of Gly and the red sphere representing the  $C=O$  carbonyl oxygen. (E) The QM-simulated IR spectrum of a tetramer ion-channel pore, displaying the vibrational behavior of two neighboring  $A\beta$ 40 helices. (F) Deconvoluted ATR-IR spectrum of pentapeptides indicating  $C\alpha-H\cdots O$  hydrogen bond. (G) Temperature-dependent NMR spectra of pentapeptide in  $CD_3OD$ . (H) Bar diagram plot of the temperature coefficients for amino acid residues of individual pentapeptides. Adapted with permission under a Creative Commons CC-BY 4.0 from ref 104. Copyright 2023, MDPI.

accessibility between  $A\beta$ 40, AV20, and G37L.  $A\beta$ 40 exhibited a mixed pattern of solvent accessibility, with higher accessibility at the N-terminus and lower accessibility at the C-terminus (Figure 5B and C). In contrast, AV20 displayed significantly larger solvent accessibility compared to G37L. The analysis of root-mean-square fluctuation (RMSF) patterns showed that Gly residues in AV20 exhibited higher solvent accessibility, leading to structural turns and compactness. These findings suggest that the  $G \rightarrow L$  mutation in G37L influences solvent accessibility and structural transitions, potentially impacting the aggregation behavior of the peptides. MD simulations also uncovered a notable disparity in solvent dynamics between AV20 and G37L. The examination of the free energy landscape further demonstrated that AV20 exhibited a wider distribution of low-energy conformations compared to G37L (Figure 5D). Additionally, this analysis provided an independent validation of the differing water dynamics in the truncated system compared to  $A\beta$ 40, which was consistent with NMR findings.

The highly amyloidogenic core (residues 60–85) of  $\alpha$ -synuclein, the protein associated with Parkinson's disease also contain several Gly residues, including an AxxxG sequence,

which could lead to a similar molecular surface. Previously, Sakagashira et al. reported that  $S \rightarrow G$  missense mutation at position 20 of the hIAPP has been associated 4.1% of Japanese patients with type 2 diabetes and 10% of those with early onset type 2 diabetes.<sup>88</sup> Later, the S20G substitution in hIAPP was found to be more amyloidogenic and cytotoxic.<sup>89</sup> This is interesting because such mutation will lead to the occurrence of a GxxxG motif. Nonetheless, in our recent study, we uncovered an intriguing finding regarding the aggregation properties of the C-terminus of hIAPP (17–37), termed as VY21, which contains GxxxS/SxxxG motif. Our findings revealed that the aggregation process of VY21 is far more complex than a straightforward shift from random coil to  $\beta$ -sheet structure. It exhibits a diverse and intriguing free-energy landscape with multiple barriers, leading to the formation of distinct types of aggregates and varying levels of cytotoxicity. We observed that VY21 predominantly forms disordered oligomers at low temperatures without agitation, while agitation leads to the formation of ThT-positive amyloid fibrils. Surprisingly, despite the commonly reported higher cytotoxicity of amyloid oligomers compared to fibrillar species,

VY21 oligomers showed limited toxicity in comparison to hIAPP. This reduced toxicity may be attributed to the disordered structure of these oligomers. Additionally, these oligomers can serve as potential seeds, triggering a cascade of aggregation kinetics that can induce conformational changes or alter dynamic exchange with monomeric species, potentially leading to distinct forms of amyloidosis. Moreover, VY21 serves as a potent scavenger, effectively reducing the presence of toxic soluble hIAPP oligomers, and demonstrates antagonistic properties by shortening the lifetime of toxic hIAPP oligomers.

### ■ GXXXG MOTIF STABILIZES ION CHANNEL LIKE PORES THROUGH $C\alpha-H\cdots O$ INTERACTION

Several TM protein and microbial peptides have been found to actively form membrane channels, with GxxxG motifs recurring in their sequences, emphasizing their significant role in ion channel formation. For instance, the VacA protein from *Helicobacter pylori* contains three tandem GxxxG motifs within its N-terminal hydrophobic region, which are crucial for oligomerization and subsequent channel formation.<sup>79</sup> Mutations in the Gly residues within these motifs, particularly G14 and G18, have been shown to disrupt oligomerization and reduce the protein's ability to form channels, leading to decreased cytotoxicity. Interestingly, ion channel-like pore formation is also a critical step in amyloid-mediated toxicity. Amyloid-forming peptides like  $A\beta$ ,  $\alpha$ -synuclein, and hIAPP have demonstrated the ability to form ion channel-like pores in various membrane mimics.<sup>75,90–95</sup> Studies have suggested that the  $A\beta$ -membrane interaction can significantly impact the aggregation pathway, although the precise molecular mechanism of this association remains unclear. The  $A\beta$ -membrane interaction has been found to induce conformational changes in the peptide secondary structure, thereby regulating the fibrillation process.<sup>96</sup> In addition to membrane-assisted structural transition, cell membrane disruption is also a significant factor contributing to  $A\beta$  neurotoxicity.<sup>97</sup> In fact, it has been proposed that during fibrillation,  $A\beta$  monomers forms ion selective pores by aggregating on to the membrane, followed by nonspecific fragmentation of the lipid membrane in a detergent-like mode.<sup>98</sup> Moreover,  $A\beta$ -membrane binding is greatly influenced by several factors like membrane composition, charge, fluidity, and curvature.<sup>99</sup> For example, the negatively charged phospholipid DMPG has been identified to accelerate the fibrillation of  $A\beta$ .<sup>100</sup> Studies by Matsuzaki and co-workers revealed that  $A\beta$ 40 specifically interacts with GM1 and undergo conformational transition into an antiparallel  $\beta$ -sheet structure with higher toxicity than that of fibrils formed under aqueous solution.<sup>101</sup> Our group has recently demonstrated the impact of different membrane compositions on  $A\beta$ 40 aggregation at an atomic resolution.<sup>102</sup> Through a comparison between a simplified blood-brain barrier (BBB) mimic, POPC/POPG/cholesterol/GM1 (PPCG), and the native BBB composed of total brain lipid extract, we have described the molecular events underlying membrane-induced amyloid aggregation. Specifically, we have highlighted the crucial role of hydrophobic interactions between the acyl chains of lipid and amino acid residues spanning K16–K28 and I31–V36 in forming transient conformations during peptide aggregation, thereby modulating the overall aggregation dynamics. Now, the question that arises is how does the involvement of the GxxxG motif contribute to it?

According to liquid-chaperone model, amyloidogenic proteins are transported into the hydrophobic membrane core if a stable complex is formed between the polypeptide and free lipids in the aqueous phase.<sup>103</sup> This complex, due to its higher hydrophobicity compared to the individual polypeptide, can then insert into the membrane. Interestingly, the GxxxG motif plays a crucial role throughout the process. Studies have shown that the presence of the GxxxG sequence on GPA and Intrinsically disorder proteins (IDPs) play a significant role in stabilizing ion-channel-like pores through weak hydrogen bonds between  $C\alpha-H$  of an  $\alpha$ -helix and  $C=O$  of the neighboring helix. However, conflicting viewpoints exist in the literature regarding the stabilizing function of the GxxxG motif. Multiscale molecular dynamics simulations of  $A\beta$ 40 inserted into a POPC membrane revealed that the peptide self-assemble into a truncated cone-shape aggregate, causing a change in membrane curvature.<sup>104</sup> These aggregate exhibited ion-channel-like pores, facilitating the passage of water and ions across the bilayer (Figure 6A). This phenomenon is explicable through the frustrated-helix model, which attributes the change in bending radius to electrostatic repulsions among exposed hydrophilic amino acids.<sup>105</sup> Furthermore, the  $A\beta$ 40 peptides predominantly adopted  $\alpha$ -helix conformation, forming twisted dimers and trimers at an average angle of  $39^\circ \pm 5^\circ$ . The aggregate within the membrane consisted of small transmembrane subunits composed of four  $A\beta$  molecules, resembling ion channels (Figure 6B). Quantum mechanics (QM) calculations revealed an interchain interaction between residues G29 and D23, where the  $H\alpha-O=C$  distance was 3.32 Å. (Figure 6E). Intrachain interactions between Gly and other residues were also observed. Moreover, the formation of a lock between two neighboring  $\alpha$ -helices facilitated by a GxxxG motif was suggested by molecular dynamics and QM calculations.

Several pentapeptides encompassing the GxxxG motif was investigated in order to evaluate the effect of hydrophobic environment. As depicted in Figure 6F, the ATR-IR spectra exhibited a band approximately at  $2910\text{ cm}^{-1}$  across all investigated pentapeptides, indicating intermolecular interaction between the Gly of a pentapeptide with its neighboring  $C=O$  group. Temperature-dependent solution NMR study further confirmed the formation of weak hydrogen bonding in hydrophobic environment as opposed to water. The temperature coefficients for the backbone amide protons ranged from  $-4$  to  $-6$  ppb/K in  $CD_3OD$ , which can be attributed to some degree of conformation inclination resulting from the close proximity of the Gly amide proton to  $C\alpha-H\cdots O$  hydrogen bonding (Figure 6G). Hence, the GxxxG motif can induce hydrogen bonding under hydrophobic environments, regardless of the intermediary residues between these Gly. This phenomenon could be an intrinsic trait of the motif, arising from the lack of steric hindrance in the Gly residue.

### ■ GXXXG MOTIF TARGETED INHIBITORS

The aggregation of  $A\beta$  peptides into amyloid fibrils and prefibrillar intermediates is widely recognized as a key factor in AD pathogenesis. However, inhibiting  $A\beta$  aggregation have been extremely challenging. The intricate nature of  $A\beta$  aggregation, characterized by diverse intermediate forms and pathways, complicates therapeutic intervention. The persistence of polymorphism in  $A\beta$  structures, from oligomers to fibrils, correlating different phenotypes, hinders efficient drug design strategies.<sup>106</sup> Even a single amino acid substitution can

Table 1. Designed Peptide Inhibitors Based on Crucial Sequence Motifs in A $\beta$ 

s. no.	peptide inhibitors	target motif/structure	ref
1.	Ac-QKLVFF-NH <sub>2</sub>	designed based on CHC and acts as $\beta$ -sheet breaker	120
2.	KLVFFKKKK, KLVFFEEEE	designed based on CHC and acts as $\beta$ -sheet breaker	142
3.	RYYAAFFARR	target an extended region (A $\beta$ (11–23)) mainly through hydrophobic and electrostatic interactions and hydrogen bonding interactions.	143
4.	iA $\beta$ 5 (LPFFD), iA $\beta$ 11 (RDLPPFPVRID)	act as $\beta$ -sheet breaker and disassembles preformed fibrils	128,144
5.	Ac-LPFFN-NH <sub>2</sub>	acts as a stabilizer of the native and nonaggregative $\alpha$ -helical conformation of A $\beta$ 40	145
6.	NAP (NAPVSIPQ)	disassembles preformed fibrils	146
7.	RG-KLVFF-GR-NH <sub>2</sub> , rG-klvff-Gr-Ac	prevent oligomerization	147,148
8.	NF11 (NAVRWSLMRPF)	targets both N-terminus and CHC, disaggregates the preformed oligomers and mature A $\beta$ fibrils	113
9.	MLRTKDLIWTLFFFLGTAVSKKRPKP-NH <sub>2</sub> , MLRTKDLIWTLFFFLGTAVSKKLVFF-NH <sub>2</sub>	designed cell-penetrating peptide derived from polycationic sequence of the PrP protein that inhibits A $\beta$ fibrillation and toxicity	149
10.	cyclo(17,21)-[Lys17,Asp21]A $\beta$ (1–28)	cyclic peptide based on CHC that disrupt A $\beta$ fibrils into nontoxic short fibrils and amorphous aggregates	150
11.	H <sub>2</sub> N-A(N-Me)FF(N-Me)VLG-Succinyl-(PEG) <sub>3</sub> -Adipoyl-G(N-Me)LV(NMe)FFA-NH <sub>2</sub>	designed hairpin-like synthetic paratope that prevents A $\beta$ fibrillation by interfering with the dock-lock mechanism	123
12.	IIGLMVGGVVIA, VVIA	based on the C-terminal A $\beta$ sequence and promotes formation of nontoxic amorphous oligomer	151
13.	GVVIA-NH <sub>2</sub> , RVVIA-NH <sub>2</sub>	based on the C-terminal A $\beta$ sequence and hinders fibril formation by complex formation	152
14.	RGTFEGKF-NH <sub>2</sub> , RGTWEGKW-NH <sub>2</sub>	targets the GxxxG motif	72,131
15.	IIGLMVG-NH <sub>2</sub>	designed based on the C-terminal A $\beta$ sequence, completely attenuates fibrillation and toxicity	153
16.	Pr-IIGL-NH <sub>2</sub> , RIIGL-NH <sub>2</sub>	designed based on the C-terminal A $\beta$ sequence, inhibits A $\beta$ 42 fibrillation and toxicity	154,155
17.	WWW, WWP, WPW, PWW	tripeptides containing Trp and Pro that tightly binds to A $\beta$ fibrils and depolymerize preformed fibrils	156

alter fibrillation kinetics and toxicity significantly. The synergy between diverse oligomers and fibrils, alongside interactions with metal ions and cellular partners, further complicates matters.<sup>107–109</sup> Targeting oligomer formation may hold promise, but a lack of high-resolution structures and the dynamic nature of these species pose significant challenges. Furthermore, the formidable blood–brain barrier impedes effective drug delivery. Efforts to develop small molecules for A $\beta$  inhibition have been stymied, as protein–protein interaction interfaces, crucial for inhibiting A $\beta$  aggregation, are notably intricate.<sup>110</sup> Protein–protein interaction regions encompass substantial surface areas, while traditional small molecule interaction regions fall short.<sup>111</sup> Additionally, these interaction surfaces lack well-defined features for small molecules to dock favorably, and the plasticity of protein surfaces can thwart inhibition.<sup>112</sup> These formidable obstacles limit the development of A $\beta$  aggregation inhibitors, rendering the task exceedingly challenging.

Nonetheless, a great number of inhibitors have been identified, designed and applied to prevent A $\beta$ -amyloidogenesis.<sup>113–119</sup> However, due to the lack of high-resolution oligomeric structures, developing specific inhibitors targeting oligomer or fibril formation have been very challenging. Some of the potent peptide-based designed inhibitors of A $\beta$  fibrillation are listed in Table 1. So far, most of the design strategies include short peptide sequence analogous to part of the native sequence of the protein or peptide responsible for fibril formation.<sup>120–122</sup> This approach is based on the fact that the short peptide fragments would self-recognize and thereby should bind to the homologous sequence in the native protein. The most popular approach for the inhibition of A $\beta$  amyloidogenesis have been the design of peptides derived from the central hydrophobic cluster (L17–A21) of A $\beta$ .<sup>123–125</sup> Since, amyloid fibrils usually adopt a cross  $\beta$ -structure, structure-based agents such as  $\beta$ -sheet breakers have also

been formulated to inhibit fibril formation.<sup>126–128</sup> These inhibitory peptides are targeted to disrupt  $\beta$ -sheets by blocking the hydrogen bond formation between  $\beta$ -strands. In addition to peptide mimics, alterations in short peptides such as N-methylation and peptide cyclization have shown enhanced conformational stability with significantly increased inhibitory effect on amyloid aggregation.<sup>129,130</sup>

The C-terminal segment of A $\beta$ , which contains GxxxG motifs, has recently been discovered to have a significant impact on amyloidosis and demonstrate toxicity. Targeting this region has emerged as a promising strategy to prevent fibril formation. Peptide-based inhibitors that specifically target the GxxxG motif have been recently developed and tested in vitro and in vivo. Interestingly, while GPA transmembrane sequence adopts an  $\alpha$ -helical conformation, the truncated GPA (70–86) peptide was found to form  $\beta$ -sheet fibrils resembling those of A $\beta$ 42.<sup>131</sup> Liu et al. identified the Gly residues G79 and G83 as key components that stabilize the sheet-to-sheet packing in the fibril structure. To disrupt this packing, they developed an 8-residue peptide, RGTFEGKF-NH<sub>2</sub>, which specifically interact with the Gly grooves on the fibril surface. The inhibitor was strategically designed to bind to the G-M-G face of GPA (70–86), with the bulky Phe side chains of the inhibitor interacting with the Gly backbone of the peptide. On the opposite face of the inhibitor, it carries charged and polar residues (R-T-E-K), intended to improve the solubility of the peptide. Later, Steven O. Smith and co-workers designed a series of peptides having alternating small and bulky residues on one face of a  $\beta$ -strand complementary to the GxMxG sequence in the C-terminus of A $\beta$  peptides.<sup>72</sup> Solid-state NMR spectroscopy confirmed that these designed inhibitors effectively disrupted the packing between the M35 residue and various Gly residues within the GxxxG motifs. Some of these inhibitor peptides demonstrated significant reduction in

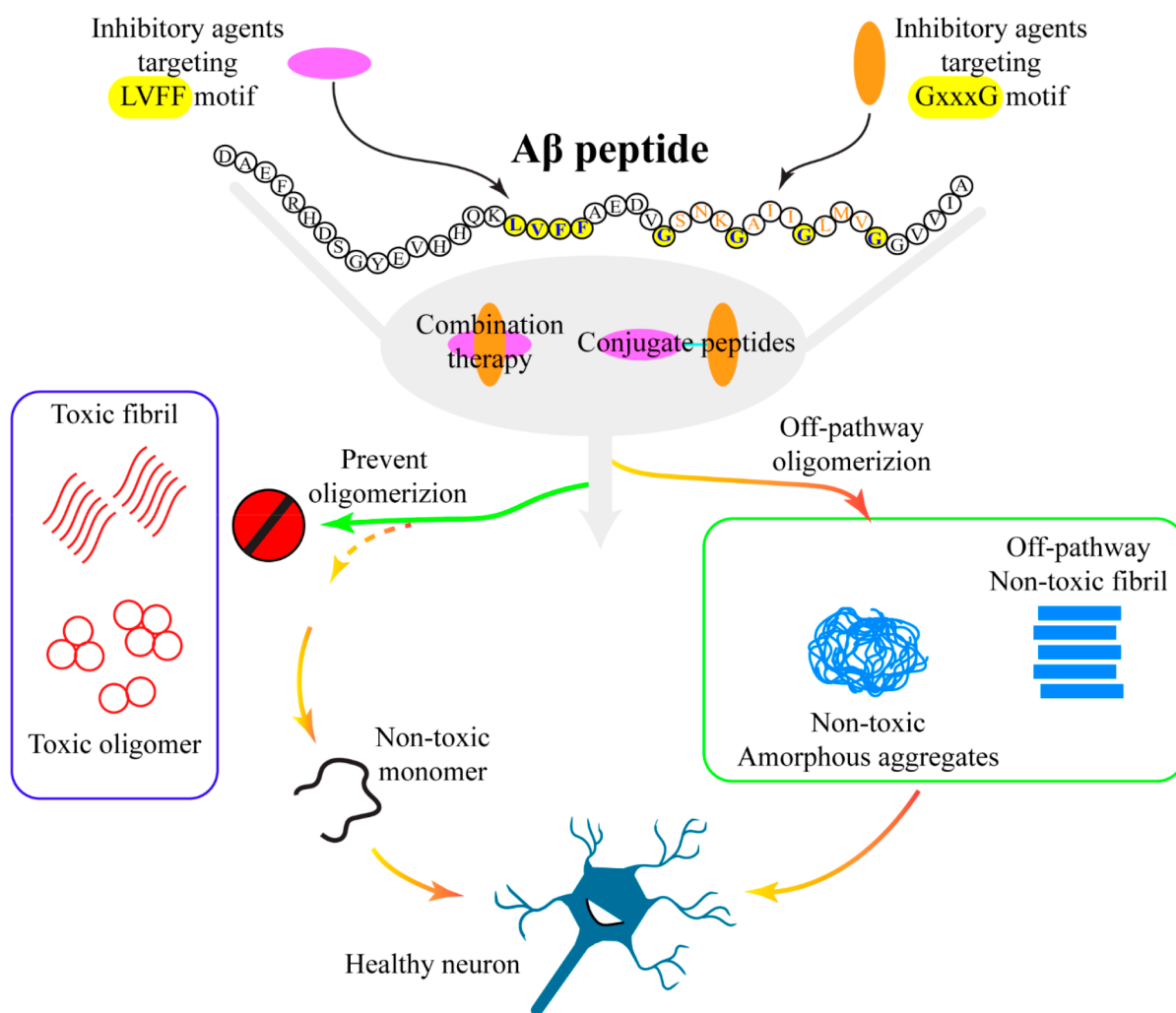


**Figure 7.** Schematic representation of amyloid inhibition targeting two most crucial sequence motifs in  $A\beta$ . Design strategies include either combination of short peptide targeting individual motifs or a conjugate peptide that can interact with both motifs. This interaction may lead to prevention of oligomerization via strong association with monomers. An alternative mechanism could involve facilitating the formation of off-pathway fibrils or amorphous aggregates that do not harm neuronal cells.

the  $A\beta_{42}$  induced toxicity on cultured rat cortical neurons, highlighting their potential therapeutic value.

Studies involving curcumin (diferulomethane) as an amyloid inhibitor have revealed its efficacy in combating both  $A\beta$  oligomers and fibrils.<sup>132</sup> Of note, the curcumin molecule possesses two aromatic groups that are separated by a  $\sim 13$  Å linker, a distance that closely aligns with the spacing between G33 and G37 of the  $A\beta$  peptides. This also holds true for several other natural products, providing possible explanations as how they act as amyloid fibril inhibitors.<sup>133</sup> Similarly, fullerene derivatives have shown remarkable potential as anti-amyloidogenic agents.<sup>134</sup> MD simulation studies have provided insights into the inhibitory mechanism, highlighting their interaction with crucial regions including the central hydrophobic cluster (CHC) represented by the LVFFA sequence, as well as the two GxxxG motifs (G<sub>29</sub>xxxG<sub>33</sub> and G<sub>33</sub>xxxG<sub>37</sub>).<sup>135</sup> Since the amyloidogenic regions of prion proteins and  $\alpha$ -synuclein contains GxxxG or AxxxG sequences that hydrogen bond in a parallel and in-register orientation, it strongly suggests that these inhibitors are likely to have broad effectiveness. Furthermore, their ability to interfere and disrupt  $\beta$ -sheet packing should complement the previously designed inhibitors that block  $\beta$ -sheet hydrogen bonding.

Recent studies have elucidated the dock-lock mechanism of fibril formation, where unstructured  $A\beta$  monomers transiently associate with the fibril surface before undergoing a slower conformational rearrangement and incorporating into the primary fibril lattice.<sup>136–139</sup> This process, involving the central K16-A21 and C-terminal M35-V40 regions, plays a critical role in fibrillation and presents a potential avenue for inhibiting amyloidosis. Remarkably, our recent investigation employing a synthetic paratope, SP1, has demonstrated selective binding to the LVFFA epitope, a crucial amyloidogenic region of  $A\beta$  peptide.<sup>123</sup> Furthermore, SP1 effectively disaggregated preformed fibrils of  $A\beta_{40}$ , leading to the formation of nontoxic species. Solution NMR analysis revealed that SP1 disrupts the essential dock-lock interactions of monomeric  $A\beta$ , suggesting molecular interference in the critical domain. Earlier studies have identified a mimotope (B6–C15) with limited resemblance to the C-terminus of  $A\beta_{42}$ , which includes GxxxG dimerization motifs.<sup>140</sup> This mimotope was combined with biotinylated TAT at the N-terminus (TAT–B6–C15), resulting in significant inhibition of  $A\beta_{42}$  fibrillation. TAT–B6–C15 also exhibited selective binding to prefibrillar  $A\beta_{42}$  oligomers, displaying no affinity for monomers, trimers, tetramers, fibrils, or ultrasonicated fragments. Moreover, it effectively countered

A $\beta$ 42-induced cytotoxicity in human SH-SY5Y neuroblastoma cells. Strategically engineered multifunctional peptide inhibitors have been developed by combining a metal-chelating unit with an antiaggregating peptidomimetic analog.<sup>141</sup> These inhibitory agents not only impede A $\beta$  aggregation but also possess the capability to chelate metal ions, offering functional prospect against A $\beta$ -metal complex formation and consequently inhibiting diverse forms of A $\beta$  aggregation pathway. Overall, these findings underscore the potential of smartly designed inhibitors as a promising therapeutic candidate against AD and other amyloidosis by selectively targeting key segments involved in amyloidogenesis.

### ■ IMPLICATIONS OF THE GXXXG MOTIF IN AD PATHOGENESIS AND THERAPEUTIC STRATEGIES

If we consider that A $\beta$  peptides or fragments of them are the main culprit in AD pathogenesis, a comprehensive roadmap of A $\beta$  pathway is very much prerequisite before going for clinical trials. While recent updates on APP processing and subsequent amyloid aggregation of A $\beta$  leading to synaptic dysfunction is alarming, the physiological function of either APP or A $\beta$  is still under investigation. It is highly plausible that A $\beta$  peptides compete with the formation of APP dimer and interfere with normal APP function. Several signal transduction mechanisms appears to be regulated by a range of enzymatic reactions, which involve a sequence of proteolytic cleavages within the lipid bilayer.<sup>50</sup> Apparently, GxxxG motif plays a significant part in the cascade of reactions, ranging from APP dimerization to stable association of  $\gamma$ -secretase complex and generation of A $\beta$  peptides.<sup>55</sup> On the basis of the experimental and computational analysis, this motif is required for certain structural and functional attributes that eventually leads to progress in amyloidosis. If this theory is correct, then designing agents that can inhibit specific interactions within the lipid bilayer becomes a priority. Although it looks very intimidating, a number of attempts have been made to inhibit the receptor functions by designing synthetic peptides that mimic portions of the target receptor.<sup>157,158</sup> Moreover, the investigation of high throughput screening for drugs targeting APP dimerization, with the aim of reducing A $\beta$  production, has also been undertaken.<sup>159</sup> Apart from that, research targeting the A $\beta$  amyloidogenic pathway has been consistent. On the basis of the experimental evidence, it can be conjectured that polymorphic fibrils or transient oligomers are the main toxic entities. Interestingly, both in vitro and in vivo data demonstrate that the GxxxG motif, particularly the G<sub>33xxx</sub>G<sub>37</sub> is crucial for prolonging certain oligomeric conformers. Evidently, these conformers need to be thoroughly characterized to develop inhibitory agents. We expect that upcoming research efforts will strongly focus on the inhibition and degradation of such deleterious oligomers. Current knowledge of short peptide design with increased specificity and effectiveness will surely come handy on this journey of unwinding A $\beta$  entanglement. Furthermore, since G33 or G37 mutants of A $\beta$  give rise to fibrils that are surprisingly nontoxic to the neuronal cells, we propose that developing short peptide derivatives (Figure 7) which may facilitate such fibril formation would presumably open up novel avenues for AD treatment.

### ■ CONCLUSIONS

In conclusion, our review focuses on the role of a common structural TM motif in APP, the GxxxG motif and its

downstream involvements in A $\beta$  pathway. It is clear that the Gly residues in this motif are highly conserved, playing a significant role from structural aspect and providing compact packing. Although there is still much to uncover regarding the precise role of this motif in APP processing, the salient features in regulating A $\beta$  oligomer formation and subsequent neurotoxicity are undeniable. High-resolution structural information on such conformers, whether it is implicated in ion channel formation or membrane disruption, will tremendously improve our understanding on the mechanism of amyloidosis. Although it offers an intriguing possibility for AD treatments, targeting the GxxxG motif within A $\beta$  presents significant challenges. The ubiquity of the GxxxG motif across transmembrane proteins signifies that disrupting GxxxG-mediated interactions could inadvertently perturb normal protein-protein interactions, potentially yielding unintended off-target effects. Furthermore, the structural polymorphism inherent to this motif complicates the design of effective inhibitors. These intricacies are compounded by the presence of other pivotal motifs within A $\beta$  and the dynamic, adaptable nature of its oligomerization process. Thus, while the GxxxG motif represents a tantalizing target, a comprehensive assessment of these limitations is essential to ensure both the safety and efficacy of therapeutic strategies. Nonetheless, this understanding will lay the groundwork for the development of potent inhibitors for future therapeutic interventions. Overall, investigating the GxxxG motif may open up exciting prospects for unraveling the complexities of protein folding disorders and advancing our ability to target them effectively.

### ■ AUTHOR INFORMATION

#### Corresponding Author

Anirban Bhunia – Department of Chemical Sciences, Bose Institute, Kolkata 700 091, India; [orcid.org/0000-0002-8752-2842](https://orcid.org/0000-0002-8752-2842); Phone: (+91) (33) 2569 3291; Email: [anirbanbhunia@gmail.com](mailto:anirbanbhunia@gmail.com), [bhunias@jcbse.ac.in](mailto:bhunias@jcbse.ac.in)

#### Author

Dibakar Sarkar – Department of Chemical Sciences, Bose Institute, Kolkata 700 091, India

Complete contact information is available at: <https://pubs.acs.org/10.1021/acsbiomedchemau.3c00055>

#### Author Contributions

CRediT: Dibakar Sarkar writing-original draft, writing-review & editing; Anirban Bhunia conceptualization, funding acquisition, supervision, writing-review & editing.

#### Notes

The authors declare no competing financial interest.

### ■ ACKNOWLEDGMENTS

This work was partly supported by Department of Biotechnology (BT/PR29978/MED/30/2037/2018 to AB) Govt. of India and partly by Bose Institute intramural extramural research fund (R/16/19/1615 to AB). D.S. would like to thanks DST-INSPIRE (Govt. of India) for providing research fellowship.

### ■ REFERENCES

(1) Lane, C. A.; Hardy, J.; Schott, J. M. Alzheimer's disease. *Eur. J. Neurol* **2018**, *25*, 59–70.

- (2) Grand, J. H.; Caspar, S.; Macdonald, S. W. Clinical features and multidisciplinary approaches to dementia care. *J. Multidiscip Healthc* **2011**, *4*, 125–147.
- (3) Sipe, J. D.; Benson, M. D.; Buxbaum, J. N.; Ikeda, S.; Merlini, G.; Saraiva, M. J.; Westermarck, P. Amyloid fibril protein nomenclature: 2010 recommendations from the nomenclature committee of the International Society of Amyloidosis. *Amyloid* **2010**, *17* (3–4), 101–104.
- (4) Murphy, M. P.; LeVine, H. Alzheimer's disease and the amyloid-beta peptide. *J. Alzheimers Dis* **2010**, *19* (1), 311–323.
- (5) Serrano-Pozo, A.; Frosch, M. P.; Masliah, E.; Hyman, B. T. Neuropathological alterations in Alzheimer disease. *Cold Spring Harb Perspect Med* **2011**, *1* (1), a006189.
- (6) Chen, G. F.; Xu, T. H.; Yan, Y.; Zhou, Y. R.; Jiang, Y.; Melcher, K.; Xu, H. E. Amyloid beta: structure, biology and structure-based therapeutic development. *Acta Pharmacol Sin* **2017**, *38* (9), 1205–1235.
- (7) Rajasekhar, K.; Chakrabarti, M.; Govindaraju, T. Function and toxicity of amyloid beta and recent therapeutic interventions targeting amyloid beta in Alzheimer's disease. *Chem. Commun. (Camb)* **2015**, *51* (70), 13434–13450.
- (8) Selkoe, D. J. Cell biology of the amyloid beta-protein precursor and the mechanism of Alzheimer's disease. *Annu. Rev. Cell Biol.* **1994**, *10*, 373–403.
- (9) Zhang, H.; Ma, Q.; Zhang, Y. W.; Xu, H. Proteolytic processing of Alzheimer's  $\beta$ -amyloid precursor protein. *J. Neurochem.* **2012**, *120*, 9–21.
- (10) Eggert, S.; Paliga, K.; Soba, P.; Evin, G.; Masters, C. L.; Weidemann, A.; Beyreuther, K. The proteolytic processing of the amyloid precursor protein gene family members APLP-1 and APLP-2 involves alpha-, beta-, gamma-, and epsilon-like cleavages: modulation of APLP-1 processing by n-glycosylation. *J. Biol. Chem.* **2004**, *279* (18), 18146–18156.
- (11) De Strooper, B.; Annaert, W. Proteolytic processing and cell biological functions of the amyloid precursor protein. *J. Cell Sci.* **2000**, *113*, 1857–1870.
- (12) Yuksel, M.; Tacal, O. Trafficking and proteolytic processing of amyloid precursor protein and secretases in Alzheimer's disease development: An up-to-date review. *Eur. J. Pharmacol.* **2019**, *856*, 172415.
- (13) Walsh, D. M.; Selkoe, D. J. A beta oligomers - a decade of discovery. *J. Neurochem* **2007**, *101* (5), 1172–1184.
- (14) Sahoo, B. R.; Cox, S. J.; Ramamoorthy, A. High-resolution probing of early events in amyloid- $\beta$  aggregation related to Alzheimer's disease. *Chem. Commun. (Camb)* **2020**, *56* (34), 4627–4639.
- (15) Benilova, I.; Karran, E.; De Strooper, B. The toxic A $\beta$  oligomer and Alzheimer's disease: an emperor in need of clothes. *Nat. Neurosci* **2012**, *15* (3), 349–357.
- (16) Glabe, C. G. Structural classification of toxic amyloid oligomers. *J. Biol. Chem.* **2008**, *283* (44), 29639–29643.
- (17) Hubin, E.; van Nuland, N. A.; Broersen, K.; Pauwels, K. Transient dynamics of A $\beta$  contribute to toxicity in Alzheimer's disease. *Cell. Mol. Life Sci.* **2014**, *71* (18), 3507–3521.
- (18) Klein, W. L.; Krafft, G. A.; Finch, C. E. Targeting small Abeta oligomers: the solution to an Alzheimer's disease conundrum? *Trends Neurosci* **2001**, *24* (4), 219–224.
- (19) Shea, D.; Hsu, C. C.; Bi, T. M.; Paranjapye, N.; Childers, M. C.; Cochran, J.; Tomberlin, C. P.; Wang, L.; Paris, D.; Zonderman, J.; et al.  $\alpha$ -Sheet secondary structure in amyloid  $\beta$ -peptide drives aggregation and toxicity in Alzheimer's disease. *Proc. Natl. Acad. Sci. U. S. A.* **2019**, *116* (18), 8895–8900.
- (20) Colletier, J. P.; Laganowsky, A.; Landau, M.; Zhao, M.; Soriaga, A. B.; Goldschmidt, L.; Flot, D.; Cascio, D.; Sawaya, M. R.; Eisenberg, D. Molecular basis for amyloid-beta polymorphism. *Proc. Natl. Acad. Sci. U. S. A.* **2011**, *108* (41), 16938–16943.
- (21) Tycko, R. Amyloid polymorphism: structural basis and neurobiological relevance. *Neuron* **2015**, *86* (3), 632–645.
- (22) Elkins, M. R.; Wang, T.; Nick, M.; Jo, H.; Lemmin, T.; Prusiner, S. B.; DeGrado, W. F.; Stöhr, J.; Hong, M. Structural Polymorphism of Alzheimer's  $\beta$ -Amyloid Fibrils as Controlled by an E22 Switch: A Solid-State NMR Study. *J. Am. Chem. Soc.* **2016**, *138* (31), 9840–9852.
- (23) Ghosh, U.; Yau, W. M.; Collinge, J.; Tycko, R. Structural differences in amyloid- $\beta$  fibrils from brains of nondemented elderly individuals and Alzheimer's disease patients. *Proc. Natl. Acad. Sci. U. S. A.* **2021**, *118* (45) DOI: 10.1073/pnas.2111863118.
- (24) Pedersen, J. S.; Andersen, C. B.; Otzen, D. E. Amyloid structure-one but not the same: the many levels of fibrillar polymorphism. *FEBS J.* **2010**, *277* (22), 4591–4601.
- (25) Kleiger, G.; Grothe, R.; Mallick, P.; Eisenberg, D. GXXXG and AXXXA: common alpha-helical interaction motifs in proteins, particularly in extremophiles. *Biochemistry* **2002**, *41* (19), 5990–5997.
- (26) Russ, W. P.; Engelman, D. M. The GxxxG motif: a framework for transmembrane helix-helix association. *J. Mol. Biol.* **2000**, *296* (3), 911–919.
- (27) Senes, A.; Gerstein, M.; Engelman, D. M. Statistical analysis of amino acid patterns in transmembrane helices: the GxxxG motif occurs frequently and in association with beta-branched residues at neighboring positions. *J. Mol. Biol.* **2000**, *296* (3), 921–936.
- (28) Arselin, G.; Giraud, M. F.; Dautant, A.; Vaillier, J.; Brèthes, D.; Couly-Salin, B.; Schaeffer, J.; Velours, J. The GxxxG motif of the transmembrane domain of subunit e is involved in the dimerization/oligomerization of the yeast ATP synthase complex in the mitochondrial membrane. *Eur. J. Biochem.* **2003**, *270* (8), 1875–1884.
- (29) Furthmayr, H.; Marchesi, V. T. Subunit structure of human erythrocyte glycoporphin A. *Biochemistry* **1976**, *15* (5), 1137–1144.
- (30) MacKenzie, K. R.; Prestegard, J. H.; Engelman, D. M. A transmembrane helix dimer: structure and implications. *Science* **1997**, *276* (5309), 131–133.
- (31) Lemmon, M. A.; Flanagan, J. M.; Treutlein, H. R.; Zhang, J.; Engelman, D. M. Sequence specificity in the dimerization of transmembrane alpha-helices. *Biochemistry* **1992**, *31* (51), 12719–12725.
- (32) Lawrie, C. M.; Sulistijo, E. S.; MacKenzie, K. R. Intermonomer hydrogen bonds enhance GxxxG-driven dimerization of the BNIP3 transmembrane domain: roles for sequence context in helix-helix association in membranes. *J. Mol. Biol.* **2010**, *396* (4), 924–936.
- (33) Bocharov, E. V.; Pustovalova, Y. E.; Pavlov, K. V.; Volynsky, P. E.; Goncharuk, M. V.; Ermolyuk, Y. S.; Karpunin, D. V.; Schulga, A. A.; Kirpichnikov, M. P.; Efremov, R. G.; et al. Unique dimeric structure of BNIP3 transmembrane domain suggests membrane permeabilization as a cell death trigger. *J. Biol. Chem.* **2007**, *282* (22), 16256–16266.
- (34) Mueller, B. K.; Subramaniam, S.; Senes, A. A frequent, GxxxG-mediated, transmembrane association motif is optimized for the formation of interhelical C $\alpha$ -H hydrogen bonds. *Proc. Natl. Acad. Sci. U. S. A.* **2014**, *111* (10), E888–895.
- (35) Palatini, M.; Müller, S. F.; Lowjaga, K. A. A. T.; Noppes, S.; Alber, J.; Lehmann, F.; Goldmann, N.; Glebe, D.; Geyer, J. Mutational Analysis of the GXXXG/A Motifs in the Human Na. *Front Mol. Biosci* **2021**, *8*, 699443.
- (36) King, G.; Dixon, A. M. Evidence for role of transmembrane helix-helix interactions in the assembly of the Class II major histocompatibility complex. *Mol. Biosyst* **2010**, *6* (9), 1650–1661.
- (37) Drake, L. A.; Drake, J. R. A triad of molecular regions contribute to the formation of two distinct MHC class II conformers. *Mol. Immunol* **2016**, *74*, 59–70.
- (38) Drake, L. A.; Hahn, A. B.; Dixon, A. M.; Drake, J. R. Differential pairing of transmembrane domain GxxxG dimerization motifs defines two HLA-DR MHC class II conformers. *J. Biol. Chem.* **2023**, *299* (7), 104869.
- (39) Coles, M.; Bicknell, W.; Watson, A. A.; Fairlie, D. P.; Craik, D. J. Solution structure of amyloid beta-peptide(1–40) in a water-micelle environment. Is the membrane-spanning domain where we think it is? *Biochemistry* **1998**, *37* (31), 11064–11077.

- (40) Shao, H.; Jao, S.; Ma, K.; Zagorski, M. G. Solution structures of micelle-bound amyloid beta-(1–40) and beta-(1–42) peptides of Alzheimer's disease. *J. Mol. Biol.* **1999**, *285* (2), 755–773.
- (41) Isbert, S.; Wagner, K.; Eggert, S.; Schweitzer, A.; Multhaup, G.; Weggen, S.; Kins, S.; Pietrzik, C. U. APP dimer formation is initiated in the endoplasmic reticulum and differs between APP isoforms. *Cell. Mol. Life Sci.* **2012**, *69* (8), 1353–1375.
- (42) Eggert, S.; Gonzalez, A. C.; Thomas, C.; Schilling, S.; Schwarz, S. M.; Tischer, C.; Adam, V.; Strecker, P.; Schmidt, V.; Willnow, T. E.; et al. Dimerization leads to changes in APP (amyloid precursor protein) trafficking mediated by LRP1 and SorLA. *Cell. Mol. Life Sci.* **2018**, *75* (2), 301–322.
- (43) Gorman, P. M.; Kim, S.; Guo, M.; Melnyk, R. A.; McLaurin, J.; Fraser, P. E.; Bowie, J. U.; Chakrabarty, A. Dimerization of the transmembrane domain of amyloid precursor proteins and familial Alzheimer's disease mutants. *BMC Neurosci* **2008**, *9*, 17.
- (44) Sureshbabu, N.; Kirubakaran, R.; Jayakumar, R. Surfactant-induced conformational transition of amyloid beta-peptide. *Eur. Biophys J.* **2009**, *38* (4), 355–367.
- (45) O'Brien, R. J.; Wong, P. C. Amyloid precursor protein processing and Alzheimer's disease. *Annu. Rev. Neurosci.* **2011**, *34*, 185–204.
- (46) García-González, L.; Pilat, D.; Baranger, K.; Rivera, S. Emerging Alternative Proteinases in APP Metabolism and Alzheimer's Disease Pathogenesis: A Focus on MT1-MMP and MT5-MMP. *Front Aging Neurosci* **2019**, *11*, 244.
- (47) Andrew, R. J.; Kellett, K. A.; Thinakaran, G.; Hooper, N. M. A Greek Tragedy: The Growing Complexity of Alzheimer Amyloid Precursor Protein Proteolysis. *J. Biol. Chem.* **2016**, *291* (37), 19235–19244.
- (48) Zhang, X.; Li, Y.; Xu, H.; Zhang, Y. W. The  $\gamma$ -secretase complex: from structure to function. *Front Cell Neurosci* **2014**, *8*, 427.
- (49) De Strooper, B.; Iwatsubo, T.; Wolfe, M. S. Presenilins and  $\gamma$ -secretase: structure, function, and role in Alzheimer Disease. *Cold Spring Harb Perspect Med.* **2012**, *2* (1), a006304.
- (50) Marchesi, V. T. An alternative interpretation of the amyloid Abeta hypothesis with regard to the pathogenesis of Alzheimer's disease. *Proc. Natl. Acad. Sci. U. S. A.* **2005**, *102* (26), 9093–9098.
- (51) Munter, L. M.; Voigt, P.; Harmeier, A.; Kaden, D.; Gottschalk, K. E.; Weise, C.; Pipkorn, R.; Schaefer, M.; Langosch, D.; Multhaup, G. GxxxG motifs within the amyloid precursor protein transmembrane sequence are critical for the etiology of Abeta42. *EMBO J.* **2007**, *26* (6), 1702–1712.
- (52) Chen, S. Y.; Zacharias, M. An internal docking site stabilizes substrate binding to  $\gamma$ -secretase: Analysis by molecular dynamics simulations. *Biophys. J.* **2022**, *121* (12), 2330–2344.
- (53) Mao, G.; Tan, J.; Cui, M. Z.; Chui, D.; Xu, X. The GxxxG motif in the transmembrane domain of AbetaPP plays an essential role in the interaction of CTF beta with the gamma-secretase complex and the formation of amyloid-beta. *J. Alzheimers Dis* **2009**, *18* (1), 167–176.
- (54) Araki, W.; Saito, S.; Takahashi-Sasaki, N.; Shiraishi, H.; Komano, H.; Murayama, K. S. Characterization of APH-1 mutants with a disrupted transmembrane GxxxG motif. *J. Mol. Neurosci* **2006**, *29* (1), 35–43.
- (55) Lee, S. F.; Shah, S.; Yu, C.; Wigley, W. C.; Li, H.; Lim, M.; Pedersen, K.; Han, W.; Thomas, P.; Lundkvist, J.; et al. A conserved GXXXG motif in APH-1 is critical for assembly and activity of the gamma-secretase complex. *J. Biol. Chem.* **2004**, *279* (6), 4144–4152.
- (56) Kienlen-Campard, P.; Tasiaux, B.; Van Hees, J.; Li, M.; Huysseune, S.; Sato, T.; Fei, J. Z.; Aimoto, S.; Courttoy, P. J.; Smith, S. O.; et al. Amyloidogenic processing but not amyloid precursor protein (APP) intracellular C-terminal domain production requires a precisely oriented APP dimer assembled by transmembrane GXXXG motifs. *J. Biol. Chem.* **2008**, *283* (12), 7733–7744.
- (57) Levy, E.; Carman, M. D.; Fernandez-Madrid, I. J.; Power, M. D.; Lieberburg, I.; van Duinen, S. G.; Bots, G. T.; Luyendijk, W.; Frangione, B. Mutation of the Alzheimer's disease amyloid gene in hereditary cerebral hemorrhage, Dutch type. *Science* **1990**, *248* (4959), 1124–1126.
- (58) Grabowski, T. J.; Cho, H. S.; Vonsattel, J. P.; Rebeck, G. W.; Greenberg, S. M. Novel amyloid precursor protein mutation in an Iowa family with dementia and severe cerebral amyloid angiopathy. *Ann. Neurol.* **2001**, *49* (6), 697–705.
- (59) Hendriks, L.; van Duijn, C. M.; Cras, P.; Cruts, M.; Van Hul, W.; van Harskamp, F.; Warren, A.; McInnis, M. G.; Antonarakis, S. E.; Martin, J.-J.; Hofman, A.; Van Broeckhoven, C. Presenile dementia and cerebral haemorrhage linked to a mutation at codon 692 of the beta-amyloid precursor protein gene. *Nat. Genet.* **1992**, *1* (3), 218–221.
- (60) Kamino, K.; Orr, H. T.; Payami, H.; Wijsman, E. M.; Alonso, M. E.; Pulst, S. M.; Anderson, L.; O'dahl, S.; Nemens, E.; White, J. A. Linkage and mutational analysis of familial Alzheimer disease kindreds for the APP gene region. *Am. J. Hum. Genet.* **1992**, *51* (5), 998–1014.
- (61) De Jonghe, C.; Zehr, C.; Yager, D.; Prada, C. M.; Younkin, S.; Hendriks, L.; Van Broeckhoven, C.; Eckman, C. B. Flemish and Dutch mutations in amyloid beta precursor protein have different effects on amyloid beta secretion. *Neurobiol Dis* **1998**, *5* (4), 281–286.
- (62) Tang, T. C.; Hu, Y.; Kienlen-Campard, P.; El Haylani, L.; Decock, M.; Van Hees, J.; Fu, Z.; Octave, J. N.; Constantinescu, S. N.; Smith, S. O. Conformational changes induced by the A21G Flemish mutation in the amyloid precursor protein lead to increased A $\beta$  production. *Structure* **2014**, *22* (3), 387–396.
- (63) Minor, D. L.; Kim, P. S. Measurement of the beta-sheet-forming propensities of amino acids. *Nature* **1994**, *367* (6464), 660–663.
- (64) Higashide, H.; Ishihara, S.; Nobuhara, M.; Ihara, Y.; Funamoto, S. Alanine substitutions in the GXXXG motif alter C99 cleavage by  $\gamma$ -secretase but not its dimerization. *J. Neurochem* **2017**, *140* (6), 955–962.
- (65) Benzinger, T. L.; Gregory, D. M.; Burkoth, T. S.; Miller-Auer, H.; Lynn, D. G.; Botto, R. E.; Meredith, S. C. Propagating structure of Alzheimer's beta-amyloid(10–35) is parallel beta-sheet with residues in exact register. *Proc. Natl. Acad. Sci. U. S. A.* **1998**, *95* (23), 13407–13412.
- (66) Groveman, B. R.; Dolan, M. A.; Taubner, L. M.; Kraus, A.; Wickner, R. B.; Caughey, B. Parallel in-register intermolecular  $\beta$ -sheet architectures for prion-seeded prion protein (PrP) amyloids. *J. Biol. Chem.* **2014**, *289* (35), 24129–24142.
- (67) Gorkovskiy, A.; Thurber, K. R.; Tycko, R.; Wickner, R. B. Locating folds of the in-register parallel  $\beta$ -sheet of the Sup35p prion domain infectious amyloid. *Proc. Natl. Acad. Sci. U. S. A.* **2014**, *111* (43), E4615–4622.
- (68) Antzutkin, O. N.; Balbach, J. J.; Leapman, R. D.; Rizzo, N. W.; Reed, J.; Tycko, R. Multiple quantum solid-state NMR indicates a parallel, not antiparallel, organization of beta-sheets in Alzheimer's beta-amyloid fibrils. *Proc. Natl. Acad. Sci. U. S. A.* **2000**, *97* (24), 13045–13050.
- (69) Antzutkin, O. N.; Balbach, J. J.; Tycko, R. Site-specific identification of non-beta-strand conformations in Alzheimer's beta-amyloid fibrils by solid-state NMR. *Biophys. J.* **2003**, *84* (5), 3326–3335.
- (70) Petkova, A. T.; Ishii, Y.; Balbach, J. J.; Antzutkin, O. N.; Leapman, R. D.; Delaglio, F.; Tycko, R. A structural model for Alzheimer's beta-amyloid fibrils based on experimental constraints from solid state NMR. *Proc. Natl. Acad. Sci. U. S. A.* **2002**, *99* (26), 16742–16747.
- (71) Ahmed, M.; Davis, J.; Aucoin, D.; Sato, T.; Ahuja, S.; Aimoto, S.; Elliott, J. I.; Van Nostrand, W. E.; Smith, S. O. Structural conversion of neurotoxic amyloid-beta(1–42) oligomers to fibrils. *Nat. Struct. Mol. Biol.* **2010**, *17* (5), 561–567.
- (72) Sato, T.; Kienlen-Campard, P.; Ahmed, M.; Liu, W.; Li, H.; Elliott, J. I.; Aimoto, S.; Constantinescu, S. N.; Octave, J. N.; Smith, S. O. Inhibitors of amyloid toxicity based on beta-sheet packing of Abeta40 and Abeta42. *Biochemistry* **2006**, *45* (17), 5503–5516.

- (73) Grasso, G.; Leanza, L.; Morbiducci, U.; Danani, A.; Deriu, M. A. Aminoacid substitutions in the glycine zipper affect the conformational stability of amyloid beta fibrils. *J. Biomol Struct Dyn* **2020**, *38* (13), 3908–3915.
- (74) Cohen, F. E.; Prusiner, S. B. Pathologic conformations of prion proteins. *Annu. Rev. Biochem.* **1998**, *67*, 793–819.
- (75) Quist, A.; Doudevski, I.; Lin, H.; Azimova, R.; Ng, D.; Frangione, B.; Kagan, B.; Ghiso, J.; Lal, R. Amyloid ion channels: a common structural link for protein-misfolding disease. *Proc. Natl. Acad. Sci. U. S. A.* **2005**, *102* (30), 10427–10432.
- (76) Lin, H.; Bhatia, R.; Lal, R. Amyloid beta protein forms ion channels: implications for Alzheimer's disease pathophysiology. *FASEB J.* **2001**, *15* (13), 2433–2444.
- (77) Barnham, K. J.; Cappai, R.; Beyreuther, K.; Masters, C. L.; Hill, A. F. Delineating common molecular mechanisms in Alzheimer's and prion diseases. *Trends Biochem. Sci.* **2006**, *31* (8), 465–472.
- (78) Lin, M. C.; Mirzabekov, T.; Kagan, B. L. Channel formation by a neurotoxic prion protein fragment. *J. Biol. Chem.* **1997**, *272* (1), 44–47.
- (79) McClain, M. S.; Iwamoto, H.; Cao, P.; Vinion-Dubiel, A. D.; Li, Y.; Szabo, G.; Shao, Z.; Cover, T. L. Essential role of a GXXXG motif for membrane channel formation by *Helicobacter pylori* vacuolating toxin. *J. Biol. Chem.* **2003**, *278* (14), 12101–12108.
- (80) Martinac, B.; Saimi, Y.; Kung, C. Ion channels in microbes. *Physiol. Rev.* **2008**, *88* (4), 1449–1490.
- (81) Kim, S.; Jeon, T. J.; Oberai, A.; Yang, D.; Schmidt, J. J.; Bowie, J. U. Transmembrane glycine zippers: physiological and pathological roles in membrane proteins. *Proc. Natl. Acad. Sci. U. S. A.* **2005**, *102* (40), 14278–14283.
- (82) Hung, L. W.; Ciccotosto, G. D.; Giannakis, E.; Tew, D. J.; Perez, K.; Masters, C. L.; Cappai, R.; Wade, J. D.; Barnham, K. J. Amyloid-beta peptide (A $\beta$ ) neurotoxicity is modulated by the rate of peptide aggregation: A $\beta$  dimers and trimers correlate with neurotoxicity. *J. Neurosci.* **2008**, *28* (46), 11950–11958.
- (83) Harmeier, A.; Wozny, C.; Rost, B. R.; Munter, L. M.; Hua, H.; Georgiev, O.; Beyermann, M.; Hildebrand, P. W.; Weise, C.; Schaffner, W.; et al. Role of amyloid-beta glycine 33 in oligomerization, toxicity, and neuronal plasticity. *J. Neurosci.* **2009**, *29* (23), 7582–7590.
- (84) Minh Thu, T. T.; Huang, S. H.; Tu, L. A.; Fang, S. T.; Li, M. S.; Chen, Y. C. G37V mutation of A $\beta$ 42 induces a nontoxic ellipse-like aggregate: An in vitro and in silico study. *Neurochem. Int.* **2019**, *129*, 104512.
- (85) Fonte, V.; Dostal, V.; Roberts, C. M.; Gonzales, P.; Lacor, P.; Magrane, J.; Dingwell, N.; Fan, E. Y.; Silverman, M. A.; Stein, G. H.; Link, C. D.; et al. A glycine zipper motif mediates the formation of toxic  $\beta$ -amyloid oligomers in vitro and in vivo. *Mol. Neurodegener.* **2011**, *6* (1), 61.
- (86) Sarkar, D.; Chakraborty, I.; Condorelli, M.; Ghosh, B.; Mass, T.; Weingarh, M.; Mandal, A. K.; La Rosa, C.; Subramanian, V.; Bhunia, A. Self-Assembly and Neurotoxicity of  $\beta$ -Amyloid (21–40) Peptide Fragment: The Regulatory Role of GxxxG Motifs. *ChemMedChem.* **2020**, *15* (3), 293–301.
- (87) Chakraborty, I.; Kar, R. K.; Sarkar, D.; Kumar, S.; Maiti, N. C.; Mandal, A. K.; Bhunia, A. Solvent Relaxation NMR: A Tool for Real-Time Monitoring Water Dynamics in Protein Aggregation Landscape. *ACS Chem. Neurosci.* **2021**, *12* (15), 2903–2916.
- (88) Sakagashira, S.; Sanke, T.; Hanabusa, T.; Shimomura, H.; Ohagi, S.; Kumagaye, K. Y.; Nakajima, K.; Nanjo, K. Missense mutation of amylin gene (S20G) in Japanese NIDDM patients. *Diabetes* **1996**, *45* (9), 1279–1281.
- (89) Meier, D. T.; Entrup, L.; Templin, A. T.; Hogan, M. F.; Mellati, M.; Zraika, S.; Hull, R. L.; Kahn, S. E. The S20G substitution in hIAPP is more amyloidogenic and cytotoxic than wild-type hIAPP in mouse islets. *Diabetologia* **2016**, *59* (10), 2166–2171.
- (90) Tosatto, L.; Andrighetti, A. O.; Plotegher, N.; Antonini, V.; Tessari, I.; Ricci, L.; Bubacco, L.; Dalla Serra, M. Alpha-synuclein pore forming activity upon membrane association. *Biochim. Biophys. Acta* **2012**, *1818* (11), 2876–2883.
- (91) Rostovtseva, T. K.; Gurnev, P. A.; Protchenko, O.; Hoogerheide, D. P.; Yap, T. L.; Philpott, C. C.; Lee, J. C.; Bezrukov, S. M.  $\alpha$ -Synuclein Shows High Affinity Interaction with Voltage-dependent Anion Channel, Suggesting Mechanisms of Mitochondrial Regulation and Toxicity in Parkinson Disease. *J. Biol. Chem.* **2015**, *290* (30), 18467–18477.
- (92) Mirzabekov, T. A.; Lin, M. C.; Kagan, B. L. Pore formation by the cytotoxic islet amyloid peptide amylin. *J. Biol. Chem.* **1996**, *271* (4), 1988–1992.
- (93) Zhao, J.; Luo, Y.; Jang, H.; Yu, X.; Wei, G.; Nussinov, R.; Zheng, J. Probing ion channel activity of human islet amyloid polypeptide (amylin). *Biochim. Biophys. Acta* **2012**, *1818* (12), 3121–3130.
- (94) Lee, J.; Kim, Y. H.; Arce, F. T.; Gillman, A. L.; Jang, H.; Kagan, B. L.; Nussinov, R.; Yang, J.; Lal, R. Amyloid  $\beta$  Ion Channels in a Membrane Comprising Brain Total Lipid Extracts. *ACS Chem. Neurosci.* **2017**, *8* (6), 1348–1357.
- (95) Arispe, N.; Diaz, J. C.; Simakova, O. Abeta ion channels. Prospects for treating Alzheimer's disease with Abeta channel blockers. *Biochim. Biophys. Acta* **2007**, *1768* (8), 1952–1965.
- (96) Fatafta, H.; Kav, B.; Bundschuh, B. F.; Loschwitz, J.; Strodel, B. Disorder-to-order transition of the amyloid- $\beta$  peptide upon lipid binding. *Biophys. Chem.* **2022**, *280*, 106700.
- (97) Madhu, P.; Das, D.; Mukhopadhyay, S. Conformation-specific perturbation of membrane dynamics by structurally distinct oligomers of Alzheimer's amyloid- $\beta$  peptide. *Phys. Chem. Chem. Phys.* **2021**, *23* (16), 9686–9694.
- (98) Sciacca, M. F.; Kotler, S. A.; Brender, J. R.; Chen, J.; Lee, D. K.; Ramamoorthy, A. Two-step mechanism of membrane disruption by A $\beta$  through membrane fragmentation and pore formation. *Biophys. J.* **2012**, *103* (4), 702–710.
- (99) Korshavn, K. J.; Satriano, C.; Lin, Y.; Zhang, R.; Dulchavsky, M.; Bhunia, A.; Ivanova, M. I.; Lee, Y. H.; La Rosa, C.; Lim, M. H.; et al. Reduced Lipid Bilayer Thickness Regulates the Aggregation and Cytotoxicity of Amyloid- $\beta$ . *J. Biol. Chem.* **2017**, *292* (11), 4638–4650.
- (100) Niu, Z.; Zhao, W.; Zhang, Z.; Xiao, F.; Tang, X.; Yang, J. The molecular structure of Alzheimer  $\beta$ -amyloid fibrils formed in the presence of phospholipid vesicles. *Angew. Chem., Int. Ed. Engl.* **2014**, *53* (35), 9294–9297.
- (101) Kakio, A.; Nishimoto, S. I.; Yanagisawa, K.; Kozutsumi, Y.; Matsuzaki, K. Cholesterol-dependent formation of GM1 ganglioside-bound amyloid beta-protein, an endogenous seed for Alzheimer amyloid. *J. Biol. Chem.* **2001**, *276* (27), 24985–24990.
- (102) Bera, S.; Gayen, N.; Mohid, S. A.; Bhattacharyya, D.; Krishnamoorthy, J.; Sarkar, D.; Choi, J.; Sahoo, N.; Mandal, A. K.; Lee, D.; et al. Comparison of Synthetic Neuronal Model Membrane Mimics in Amyloid Aggregation at Atomic Resolution. *ACS Chem. Neurosci.* **2020**, *11* (13), 1965–1977.
- (103) Sciacca, M. F.; Lolicato, F.; Tempra, C.; Scollo, F.; Sahoo, B. R.; Watson, M. D.; García-Viñuales, S.; Milardi, D.; Raudino, A.; Lee, J. C.; et al. Lipid-Chaperone Hypothesis: A Common Molecular Mechanism of Membrane Disruption by Intrinsically Disordered Proteins. *ACS Chem. Neurosci.* **2020**, *11* (24), 4336–4350.
- (104) Rando, C.; Grasso, G.; Sarkar, D.; Sciacca, M. F. M.; Cucci, L. M.; Cosentino, A.; Forte, G.; Pannuzzo, M.; Satriano, C.; Bhunia, A. GxxxG Motif Stabilize Ion-Channel like Pores through C. *Int. J. Mol. Sci.* **2023**, *24* (3), 2192.
- (105) Pannuzzo, M.; Milardi, D.; Raudino, A.; Karttunen, M.; La Rosa, C. Analytical model and multiscale simulations of A $\beta$  peptide aggregation in lipid membranes: towards a unifying description of conformational transitions, oligomerization and membrane damage. *Phys. Chem. Chem. Phys.* **2013**, *15* (23), 8940–8951.
- (106) Qiang, W.; Yau, W. M.; Lu, J. X.; Collinge, J.; Tycko, R. Structural variation in amyloid- $\beta$  fibrils from Alzheimer's disease clinical subtypes. *Nature* **2017**, *541* (7636), 217–221.
- (107) Abelein, A. Metal Binding of Alzheimer's Amyloid- $\beta$  and Its Effect on Peptide Self-Assembly. *Acc. Chem. Res.* **2023**, *56*, 2653.

- (108) Faller, P.; Hureau, C.; La Penna, G. Metal ions and intrinsically disordered proteins and peptides: from Cu/Zn amyloid- $\beta$  to general principles. *Acc. Chem. Res.* **2014**, *47* (8), 2252–2259.
- (109) Lau, T. L.; Gehman, J. D.; Wade, J. D.; Perez, K.; Masters, C. L.; Barnham, K. J.; Separovic, F. Membrane interactions and the effect of metal ions of the amyloidogenic fragment A $\beta$ (25–35) in comparison to A $\beta$ (1–42). *Biochim. Biophys. Acta* **2007**, *1768* (10), 2400–2408.
- (110) Jones, S.; Thornton, J. M. Principles of protein-protein interactions. *Proc. Natl. Acad. Sci. U. S. A.* **1996**, *93* (1), 13–20.
- (111) Cheng, A. C.; Coleman, R. G.; Smyth, K. T.; Cao, Q.; Soulard, P.; Caffrey, D. R.; Salzberg, A. C.; Huang, E. S. Structure-based maximal affinity model predicts small-molecule druggability. *Nat. Biotechnol.* **2007**, *25* (1), 71–75.
- (112) Gestwicki, J. E.; Crabtree, G. R.; Graef, I. A. Harnessing chaperones to generate small-molecule inhibitors of amyloid beta aggregation. *Science* **2004**, *306* (5697), 865–869.
- (113) Ghosh, A.; Pradhan, N.; Bera, S.; Datta, A.; Krishnamoorthy, J.; Jana, N. R.; Bhunia, A. Inhibition and Degradation of Amyloid Beta (A $\beta$ 40) Fibrillation by Designed Small Peptide: A Combined Spectroscopy, Microscopy, and Cell Toxicity Study. *ACS Chem. Neurosci.* **2017**, *8* (4), 718–722.
- (114) Jokar, S.; Erfani, M.; Bavi, O.; Khazaei, S.; Sharifzadeh, M.; Hajiramezani, M.; Beiki, D.; Shamloo, A. Design of peptide-based inhibitor agent against amyloid- $\beta$  aggregation: Molecular docking, synthesis and in vitro evaluation. *Bioorg. Chem.* **2020**, *102*, 104050.
- (115) Horsley, J. R.; Jovceviski, B.; Wegener, K. L.; Yu, J.; Pukala, T. L.; Abell, A. D. Rationally designed peptide-based inhibitor of A $\beta$ 42 fibril formation and toxicity: a potential therapeutic strategy for Alzheimer's disease. *Biochem. J.* **2020**, *477* (11), 2039–2054.
- (116) Jha, A.; Kumar, M. G.; Gopi, H. N.; Paknikar, K. M. Inhibition of  $\beta$ -Amyloid Aggregation through a Designed  $\beta$ -Hairpin Peptide. *Langmuir* **2018**, *34* (4), 1591–1600.
- (117) Milojevic, J.; Esposito, V.; Das, R.; Melacini, G. Understanding the molecular basis for the inhibition of the Alzheimer's A $\beta$ -peptide oligomerization by human serum albumin using saturation transfer difference and off-resonance relaxation NMR spectroscopy. *J. Am. Chem. Soc.* **2007**, *129* (14), 4282–4290.
- (118) Choi, J. S.; Braymer, J. J.; Nanga, R. P.; Ramamoorthy, A.; Lim, M. H. Design of small molecules that target metal-A $\beta$  species and regulate metal-induced A $\beta$  aggregation and neurotoxicity. *Proc. Natl. Acad. Sci. U. S. A.* **2010**, *107* (51), 21990–21995.
- (119) Goyal, D.; Shuaib, S.; Mann, S.; Goyal, B. Rationally Designed Peptides and Peptidomimetics as Inhibitors of Amyloid- $\beta$  (A $\beta$ ) Aggregation: Potential Therapeutics of Alzheimer's Disease. *ACS Comb. Sci.* **2017**, *19* (2), 55–80.
- (120) Tjernberg, L. O.; Näslund, J.; Lindqvist, F.; Johansson, J.; Karlström, A. R.; Thyberg, J.; Terenius, L.; Nordstedt, C. Arrest of beta-amyloid fibril formation by a pentapeptide ligand. *J. Biol. Chem.* **1996**, *271* (15), 8545–8548.
- (121) Wei, C. W.; Peng, Y.; Zhang, L.; Huang, Q.; Cheng, M.; Liu, Y. N.; Li, J. Synthesis and evaluation of ferrocenoyl pentapeptide (Fc-KLVFF) as an inhibitor of Alzheimer's A $\beta$ <sub>1–42</sub> fibril formation in vitro. *Bioorg. Med. Chem. Lett.* **2011**, *21* (19), 5818–5821.
- (122) Wang, L.; Lei, L.; Li, Y.; Wang, L.; Li, F. A hIAPP-derived all-D-amino-acid inhibits hIAPP fibrillation efficiently at membrane surface by targeting  $\alpha$ -helical oligomeric intermediates. *FEBS Lett.* **2014**, *588* (6), 884–891.
- (123) Paul, A.; Kumar, S.; Kalita, S.; Kalita, S.; Sarkar, D.; Bhunia, A.; Bandyopadhyay, A.; Mondal, A. C.; Mandal, B. An explicitly designed paratope of amyloid- $\beta$  prevents neuronal apoptosis. *Chem. Sci.* **2021**, *12* (8), 2853–2862.
- (124) Castelletto, V.; Cheng, G.; Hamley, I. W. Amyloid peptides incorporating a core sequence from the amyloid beta peptide and gamma amino acids: relating bioactivity to self-assembly. *Chem. Commun. (Camb)* **2011**, *47* (46), 12470–12472.
- (125) Arai, T.; Sasaki, D.; Araya, T.; Sato, T.; Sohma, Y.; Kanai, M. A cyclic KLVFF-derived peptide aggregation inhibitor induces the formation of less-toxic off-pathway amyloid- $\beta$  oligomers. *Chembiochem* **2014**, *15* (17), 2577–2583.
- (126) Francioso, A.; Punzi, P.; Boffi, A.; Lori, C.; Martire, S.; Giordano, C.; D'Erme, M.; Mosca, L.  $\beta$ -sheet interfering molecules acting against  $\beta$ -amyloid aggregation and fibrillogenesis. *Bioorg. Med. Chem.* **2015**, *23* (8), 1671–1683.
- (127) Zhang, L.; Yagnik, G.; Peng, Y.; Wang, J.; Xu, H. H.; Hao, Y.; Liu, Y. N.; Zhou, F. Kinetic studies of inhibition of the amyloid beta (1–42) aggregation using a ferrocene-tagged  $\beta$ -sheet breaker peptide. *Anal. Biochem.* **2013**, *434* (2), 292–299.
- (128) Soto, C.; Sigurdsson, E. M.; Morelli, L.; Kumar, R. A.; Castaño, E. M.; Frangione, B. Beta-sheet breaker peptides inhibit fibrillogenesis in a rat brain model of amyloidosis: implications for Alzheimer's therapy. *Nat. Med.* **1998**, *4* (7), 822–826.
- (129) Tatak-Nossol, M.; Yan, L. M.; Schmauder, A.; Tenidis, K.; Westermarck, G.; Kapurniotu, A. Inhibition of hIAPP amyloid-fibril formation and apoptotic cell death by a designed hIAPP amyloid-core-containing hexapeptide. *Chem. Biol.* **2005**, *12* (7), 797–809.
- (130) Pariary, R.; Ghosh, B.; Bednarikova, Z.; Varnava, K. G.; Ratha, B. N.; Raha, S.; Bhattacharyya, D.; Gazova, Z.; Sarojini, V.; Mandal, A. K.; et al. Targeted inhibition of amyloidogenesis using a non-toxic, serum stable strategically designed cyclic peptide with therapeutic implications. *Biochim Biophys Acta Proteins Proteom* **2020**, *1868* (5), 140378.
- (131) Liu, W.; Crocker, E.; Zhang, W.; Elliott, J. I.; Luy, B.; Li, H.; Aimoto, S.; Smith, S. O. Structural role of glycine in amyloid fibrils formed from transmembrane alpha-helices. *Biochemistry* **2005**, *44* (9), 3591–3597.
- (132) Yang, F.; Lim, G. P.; Begum, A. N.; Ubeda, O. J.; Simmons, M. R.; Ambegaokar, S. S.; Chen, P. P.; Kayed, R.; Glabe, C. G.; Frautschy, S. A.; et al. Curcumin inhibits formation of amyloid beta oligomers and fibrils, binds plaques, and reduces amyloid in vivo. *J. Biol. Chem.* **2005**, *280* (7), 5892–5901.
- (133) Rajasekhar, K.; Samanta, S.; Bagoband, V.; Murugan, N. A.; Govindaraju, T. Antioxidant Berberine-Derivative Inhibits Multifaceted Amyloid Toxicity. *iScience* **2020**, *23* (4), 101005.
- (134) Kim, J. E.; Lee, M. Fullerene inhibits beta-amyloid peptide aggregation. *Biochem. Biophys. Res. Commun.* **2003**, *303* (2), 576–579.
- (135) Sun, Y.; Qian, Z.; Wei, G. The inhibitory mechanism of a fullerene derivative against amyloid- $\beta$  peptide aggregation: an atomistic simulation study. *Phys. Chem. Chem. Phys.* **2016**, *18* (18), 12582–12591.
- (136) Rodriguez, R. A.; Chen, L. Y.; Plascencia-Villa, G.; Perry, G. Thermodynamics of Amyloid- $\beta$  Fibril Elongation: Atomistic Details of the Transition State. *ACS Chem. Neurosci.* **2018**, *9* (4), 783–789.
- (137) Nguyen, P. H.; Li, M. S.; Stock, G.; Straub, J. E.; Thirumalai, D. Monomer adds to preformed structured oligomers of A $\beta$ -peptides by a two-stage dock-lock mechanism. *Proc. Natl. Acad. Sci. U. S. A.* **2007**, *104* (1), 111–116.
- (138) Brender, J. R.; Ghosh, A.; Kotler, S. A.; Krishnamoorthy, J.; Bera, S.; Morris, V.; Sil, T. B.; Garai, K.; Reif, B.; Bhunia, A.; et al. Probing transient non-native states in amyloid beta fiber elongation by NMR. *Chem. Commun. (Camb)* **2019**, *55* (31), 4483–4486.
- (139) Kar, R. K.; Brender, J. R.; Ghosh, A.; Bhunia, A. Nonproductive Binding Modes as a Prominent Feature of A $\beta$ . *J. Chem. Inf. Model* **2018**, *58* (8), 1576–1586.
- (140) Tanaka, K.; Nishimura, M.; Yamaguchi, Y.; Hashiguchi, S.; Takiguchi, S.; Yamaguchi, M.; Tahara, H.; Gotanda, T.; Abe, R.; Ito, Y.; et al. A mimotope peptide of A $\beta$ 42 fibril-specific antibodies with A $\beta$ 42 fibrillation inhibitory activity induces anti-A $\beta$ 42 conformer antibody response by a displayed form on an M13 phage in mice. *J. Neuroimmunol* **2011**, *236* (1–2), 27–38.
- (141) Rajasekhar, K.; Madhu, C.; Govindaraju, T. Natural Tripeptide-Based Inhibitor of Multifaceted Amyloid  $\beta$  Toxicity. *ACS Chem. Neurosci.* **2016**, *7* (9), 1300–1310.
- (142) Lowe, T. L.; Strzelec, A.; Kiessling, L. L.; Murphy, R. M. Structure-function relationships for inhibitors of beta-amyloid toxicity containing the recognition sequence KLVFF. *Biochemistry* **2001**, *40* (26), 7882–7889.

- (143) Liu, J.; Wang, W.; Zhang, Q.; Zhang, S.; Yuan, Z. Study on the efficiency and interaction mechanism of a decapeptide inhibitor of  $\beta$ -amyloid aggregation. *Biomacromolecules* **2014**, *15* (3), 931–939.
- (144) Soto, C.; Kindy, M. S.; Baumann, M.; Frangione, B. Inhibition of Alzheimer's amyloidosis by peptides that prevent beta-sheet conformation. *Biochem. Biophys. Res. Commun.* **1996**, *226* (3), 672–680.
- (145) Minicozzi, V.; Chiaraluze, R.; Consalvi, V.; Giordano, C.; Narcisi, C.; Punzi, P.; Rossi, G. C.; Morante, S. Computational and experimental studies on  $\beta$ -sheet breakers targeting A $\beta$ 1–40 fibrils. *J. Biol. Chem.* **2014**, *289* (16), 11242–11252.
- (146) Ashur-Fabian, O.; Segal-Ruder, Y.; Skutelsky, E.; Brenneman, D. E.; Steingart, R. A.; Giladi, E.; Gozes, I. The neuroprotective peptide NAP inhibits the aggregation of the beta-amyloid peptide. *Peptides* **2003**, *24* (9), 1413–1423.
- (147) Austen, B. M.; Paleologou, K. E.; Ali, S. A.; Qureshi, M. M.; Allsop, D.; El-Agnaf, O. M. Designing peptide inhibitors for oligomerization and toxicity of Alzheimer's beta-amyloid peptide. *Biochemistry* **2008**, *47* (7), 1984–1992.
- (148) Taylor, M.; Moore, S.; Mayes, J.; Parkin, E.; Beeg, M.; Canovi, M.; Gobbi, M.; Mann, D. M.; Allsop, D. Development of a proteolytically stable retro-inverso peptide inhibitor of beta-amyloid oligomerization as a potential novel treatment for Alzheimer's disease. *Biochemistry* **2010**, *49* (15), 3261–3272.
- (149) Henning-Knechtel, A.; Kumar, S.; Wallin, C.; Krol, S.; Warmlander, S. K.T.S.; Jarvet, J.; Esposito, G.; Kirmizialtin, S.; Graslund, A.; Hamilton, A. D.; Magzoub, M. Designed cell-penetrating peptide inhibitors of amyloid-beta aggregation and cytotoxicity. *Cell Rep. Phys. Sci.* **2020**, *1* (2), 100014.
- (150) Kapurniotu, A.; Buck, A.; Weber, M.; Schmauder, A.; Hirsch, T.; Bernhagen, J.; Tatarek-Nossol, M. Conformational restriction via cyclization in beta-amyloid peptide Abeta(1–28) leads to an inhibitor of Abeta(1–28) amyloidogenesis and cytotoxicity. *Chem. Biol.* **2003**, *10* (2), 149–159.
- (151) Fradinger, E. A.; Monien, B. H.; Urbanc, B.; Lomakin, A.; Tan, M.; Li, H.; Spring, S. M.; Condrion, M. M.; Cruz, L.; Xie, C. W.; et al. C-terminal peptides coassemble into Abeta42 oligomers and protect neurons against Abeta42-induced neurotoxicity. *Proc. Natl. Acad. Sci. U. S. A.* **2008**, *105* (37), 14175–14180.
- (152) Hetényi, C.; Szabó, Z.; Klement, E.; Datki, Z.; Körtvélyesi, T.; Zarándi, M.; Penke, B. Pentapeptide amides interfere with the aggregation of beta-amyloid peptide of Alzheimer's disease. *Biochem. Biophys. Res. Commun.* **2002**, *292* (4), 931–936.
- (153) Bansal, S.; Maurya, I. K.; Yadav, N.; Thota, C. K.; Kumar, V.; Tikoo, K.; Chauhan, V. S.; Jain, R. C-Terminal Fragment, A $\beta$ 32–37, Analogues Protect Against A $\beta$  Aggregation-Induced Toxicity. *ACS Chem. Neurosci.* **2016**, *7* (5), 615–623.
- (154) Harkany, T.; Abrahama, I.; Laskay, G.; Timmerman, W.; Jost, K.; Zarándi, M.; Penke, B.; Nyakas, C.; Luiten, P. G. M. Propionyl-IIGL tetrapeptide antagonizes beta-amyloid excitotoxicity in rat nucleus basalis. *NeuroReport* **1999**, *10* (8), 1693–1698.
- (155) Fülöp, L.; Zarándi, M.; Datki, Z.; Soós, K.; Penke, B. Beta-amyloid-derived pentapeptide RIIGLa inhibits Abeta(1–42) aggregation and toxicity. *Biochem. Biophys. Res. Commun.* **2004**, *324* (1), 64–69.
- (156) Viet, M. H.; Siposova, K.; Bednarikova, Z.; Antosova, A.; Nguyen, T. T.; Gazova, Z.; Li, M. S. In Silico and in Vitro Study of Binding Affinity of Tripeptides to Amyloid  $\beta$  Fibrils: Implications for Alzheimer's Disease. *J. Phys. Chem. B* **2015**, *119* (16), 5145–5155.
- (157) Lin, Y. Z.; Yao, S. Y.; Veach, R. A.; Torgerson, T. R.; Hawiger, J. Inhibition of nuclear translocation of transcription factor NF-kappa B by a synthetic peptide containing a cell membrane-permeable motif and nuclear localization sequence. *J. Biol. Chem.* **1995**, *270* (24), 14255–14258.
- (158) Manolios, N.; Collier, S.; Taylor, J.; Pollard, J.; Harrison, L. C.; Bender, V. T-cell antigen receptor transmembrane peptides modulate T-cell function and T cell-mediated disease. *Nat. Med.* **1997**, *3* (1), 84–88.
- (159) So, P. P.; Zeldich, E.; Seyb, K. I.; Huang, M. M.; Concannon, J. B.; King, G. D.; Chen, C. D.; Cuny, G. D.; Glicksman, M. A.; Abraham, C. R. Lowering of amyloid beta peptide production with a small molecule inhibitor of amyloid- $\beta$  precursor protein dimerization. *Am. J. Neurodegen. Dis.* **2012**, *1* (1), 75–87.